Bayesian Inference of Kinematic Rupture Parameters

Damiano Monelli, Institute of Geophysics, ETH Zurich

2009 SCEC Annual Meeting, Source Inversion Validation Workshop

From the Source Inversion Validation Workshop description:

…source-inversion results for past events exhibit large intra-event variability for models developed by different research teams for the same earthquake. Also, the reliability, resolution, and robustness of the inversion strategies and the obtained rupture models have not received their due attention.

Final slip distributions for the 1999 Izmit (Turkey) earthquake, (Ide et al,2005)

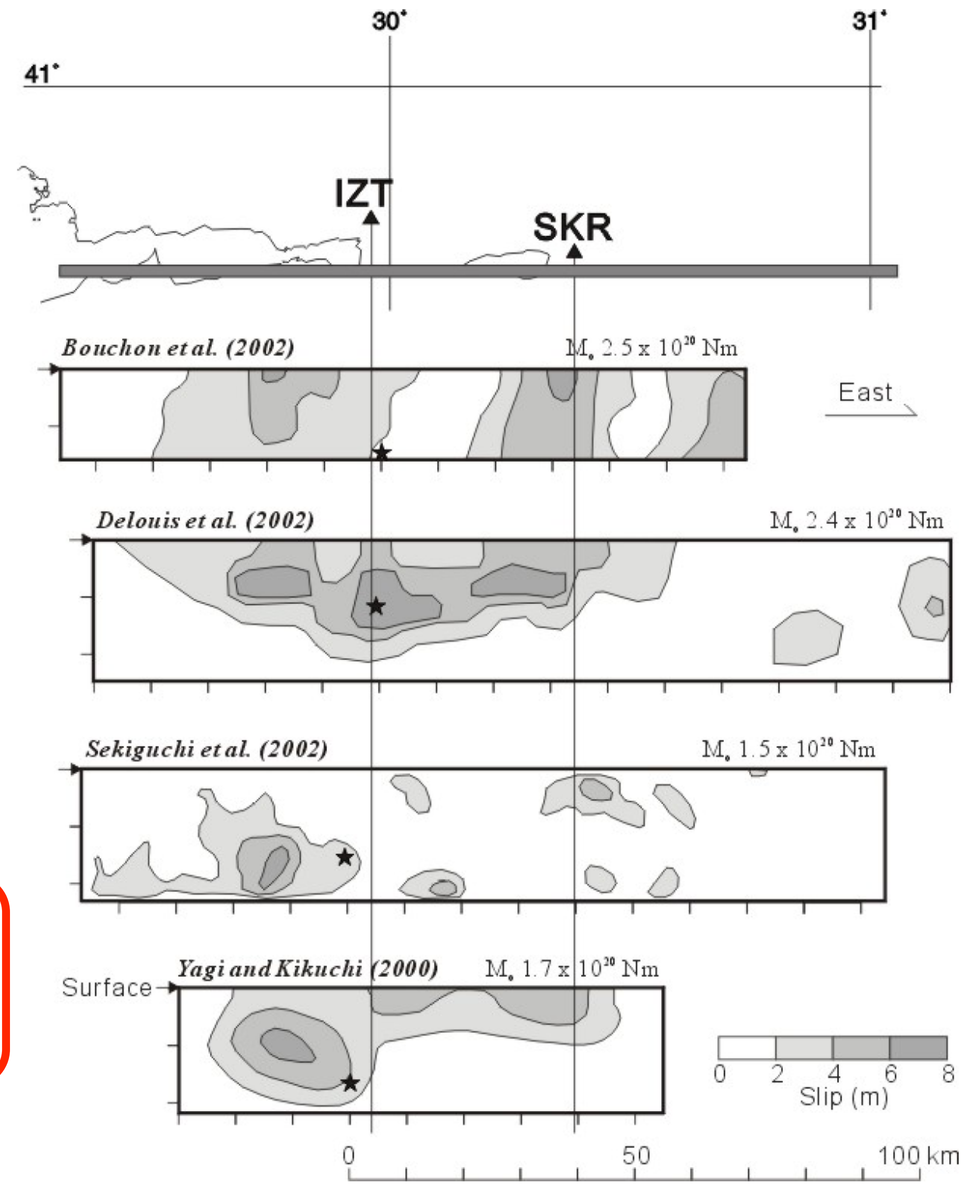

Differences can be due to:

- different modeling assumptions (fault model, fault discretization, velocity structure, data-set used, rupture parametrization (i.e. source time function),..)

- different inversion strategies (regularization method, misfit function, linear/non-linear)

- intrinsic uncertainties (uncertain data and modeling, finite data-set)

A Bayesian approach for earthquake source imaging

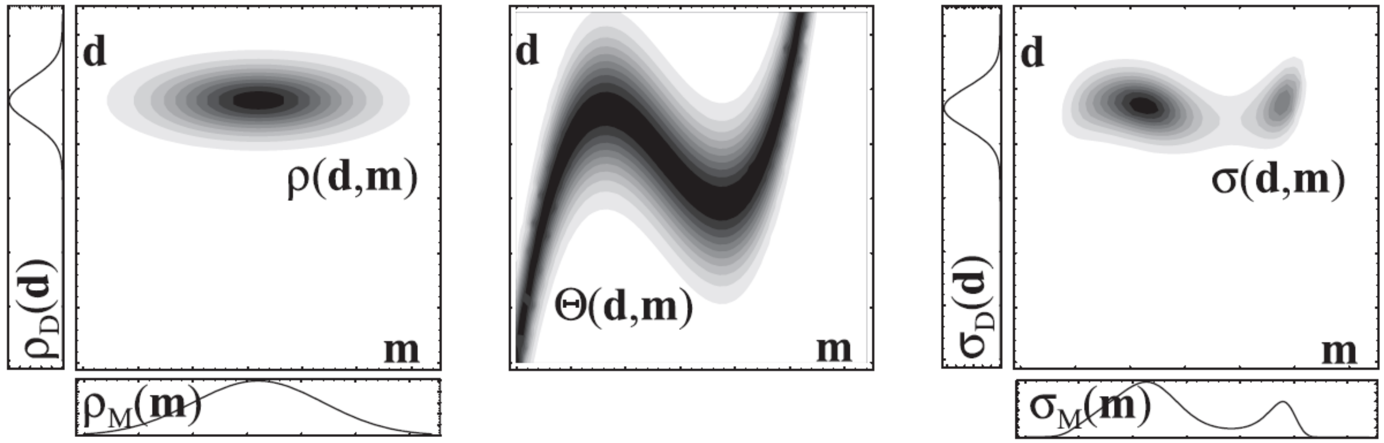

Information on data (**d**) and prior information on model parameters (**m**).

Information on the correlation between data and model parameters as predicted by a "non-exact" physical theory.

Posterior state of information

Prior PDF

Posterior PDF →

$$\sigma_M(\mathbf{m}) = k\,\rho_M(\mathbf{m})\,L(\mathbf{m})$$

← Likelihood function

1D Posterior marginal PDF →

$$M(m^\alpha) = \int \ldots \int \sigma_M(\mathbf{m}) \prod_{\substack{k=1 \\ k\neq\alpha}}^{M} dm^k$$

The prior PDF

✓ The prior knowledge consists only of the information that each model parameter is strictly bounded by two values (minimum and maximum).

$$\rho(\mathbf{m}) = \prod_{\alpha_M \in I_M} \rho_\alpha(m^\alpha)$$

$$\rho_\alpha(m^\alpha) = \begin{cases} \frac{1}{m^\alpha_{max} - m^\alpha_{min}} & \text{for } m^\alpha_{min} \leq m^\alpha \leq m^\alpha_{max} \\ 0 & \text{otherwise} \end{cases}$$

The likelihood function

✓ For Strong Motion Data

$$L^{sm}(\mathbf{m}) = \begin{cases} c & ,\forall \mathbf{m} \in \mathbb{M} : \phi(\mathbf{d}^{obs}, \mathbf{m}) < 0 \\ c \exp[-\phi(\mathbf{d}^{obs}, \mathbf{m})] & ,\forall \mathbf{m} \in \mathbb{M} : \phi(\mathbf{d}^{obs}, \mathbf{m}) \geq 0 \end{cases}$$

Misfit function (L2 norm)

$$\phi(\mathbf{d}, \mathbf{m}) = \frac{S(\mathbf{m}) - S(\mathbf{m}^{best}(\mathbf{d}))}{S(\mathbf{m}^{best}(\mathbf{d}))} \cdot 100$$

Misfit function value generated by the best-fitting model (found through optimization)

The likelihood function

✓ For GPS Data

Data covariance matrix

$$L^{gps}(\mathbf{m}) = C\exp\left[-\frac{1}{2}\mathbf{r}^T\mathbf{C}_{d,gps}^{-1}\mathbf{r}\right]$$

Residuals

$$\mathbf{r} = \mathbf{g}(\mathbf{m}) - \mathbf{d}^{obs}$$

The posterior PDF

✓ For Strong Motion data only

$$\sigma_M^{sm}(\mathbf{m}) = k\rho_M(\mathbf{m})L^{sm}(\mathbf{m})$$

✓ For Strong Motion + GPS

$$\sigma_M^{sm,gps}(\mathbf{m}) = k\rho_M(\mathbf{m})L^{sm}(\mathbf{m})L^{gps}(\mathbf{m})$$

The 2000 Western Tottori (Japan) earthquake (M_W=6.6)

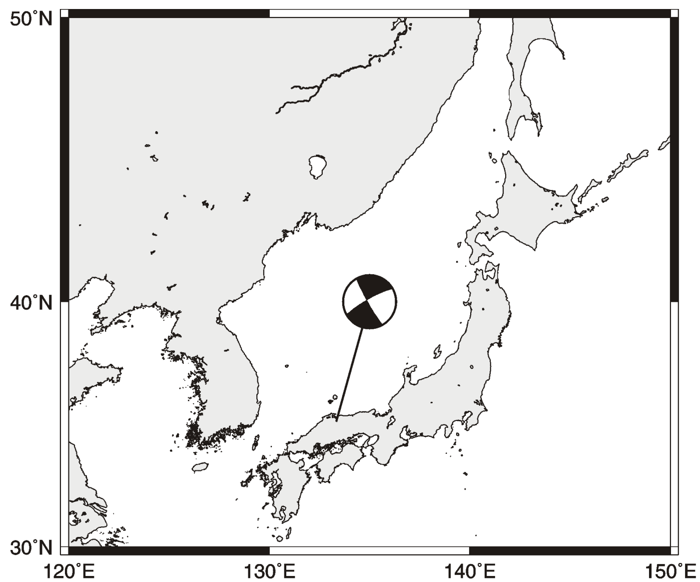

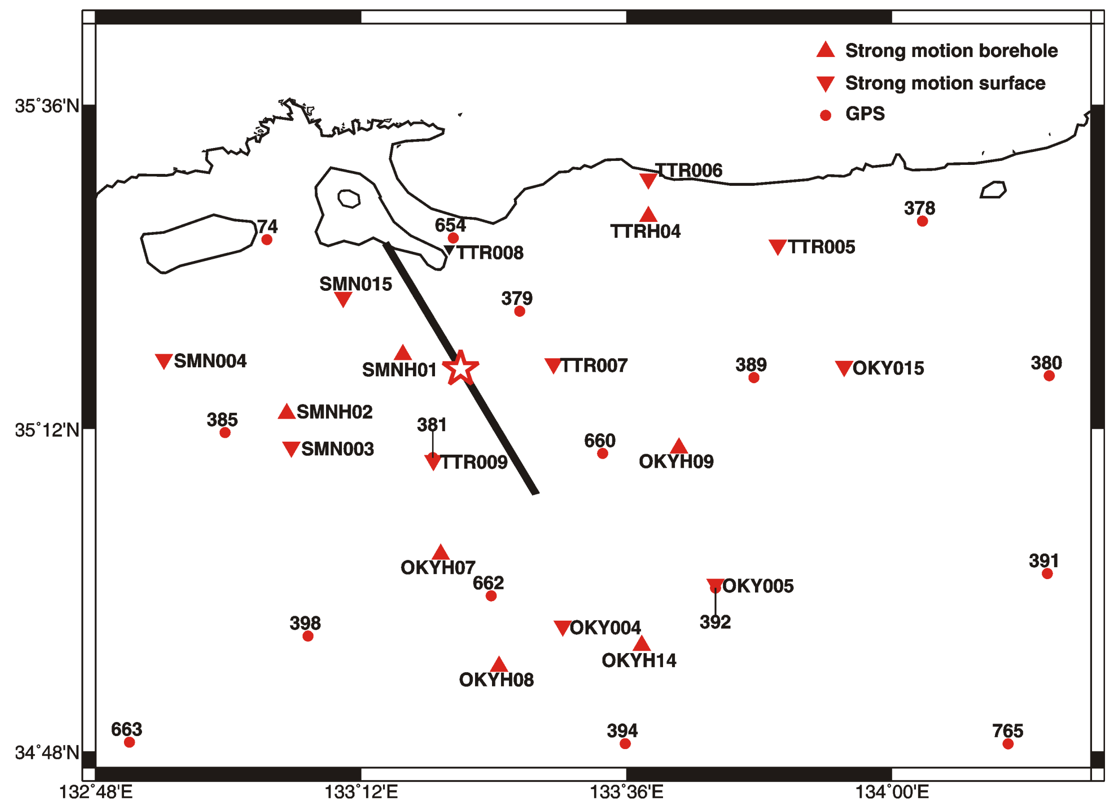

-18 Strong motion stations

-16 GPS stations

Inversion set-up (1)

The forward modeling:

✓Single planar fault (length = 40 km, width = 20 km), vertically dipping. Fault upper edge at 0.5 km depth.

✓ Rupture parameters (peak slip-velocity, rake angle, rise time, rupture time) defined on a 4 by 4 km grid. Bilinear interpolation is used to derive rupture parameters inside each grid cell.

✓ Isosceles triangle as source time function.

✓ Ground velocity (up to 1 Hz) computed with a Discrete Wavenumber / Finite Element method (Compsyn package, Spudich and Xu (2002)) for a 1D velocity model.

Inversion set-up

The model space:

✓ Peak slip-velocity can vary between 0 and 400 cm/s.

✓ Rake angle can vary between -30 to +30 degrees.

✓ Rupture time at each grid node is defined as the time interval between the arrival times of two circular rupture fronts propagating from the hypocenter at two limiting rupture velocities: 1.5 km/s and 4 km/s.

✓ The minimum rise time is equal to 1 s. The maximum rise time is assumed to be decrease approaching the fault edges.

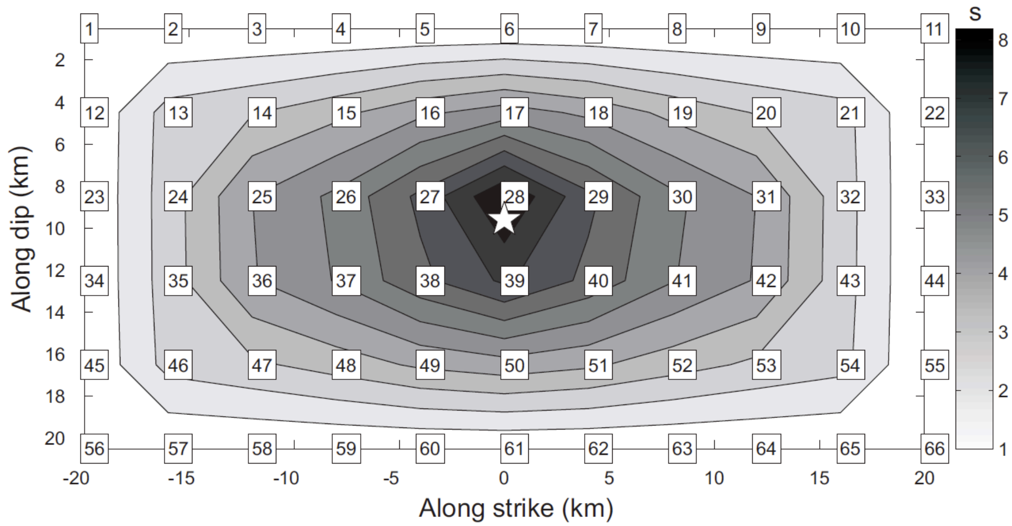

Inversion set-up

Additional constraints:

- ✓ Peak slip-velocity is assumed to be zero at the fault edges.
- ✓ Rise time is assumed to be equal to 1 s at the fault edges.

The total number of free model parameters is 204.

The computation of the marginal posterior PDFs is performed by using a MCMC method based on the Metropolis algorithm.

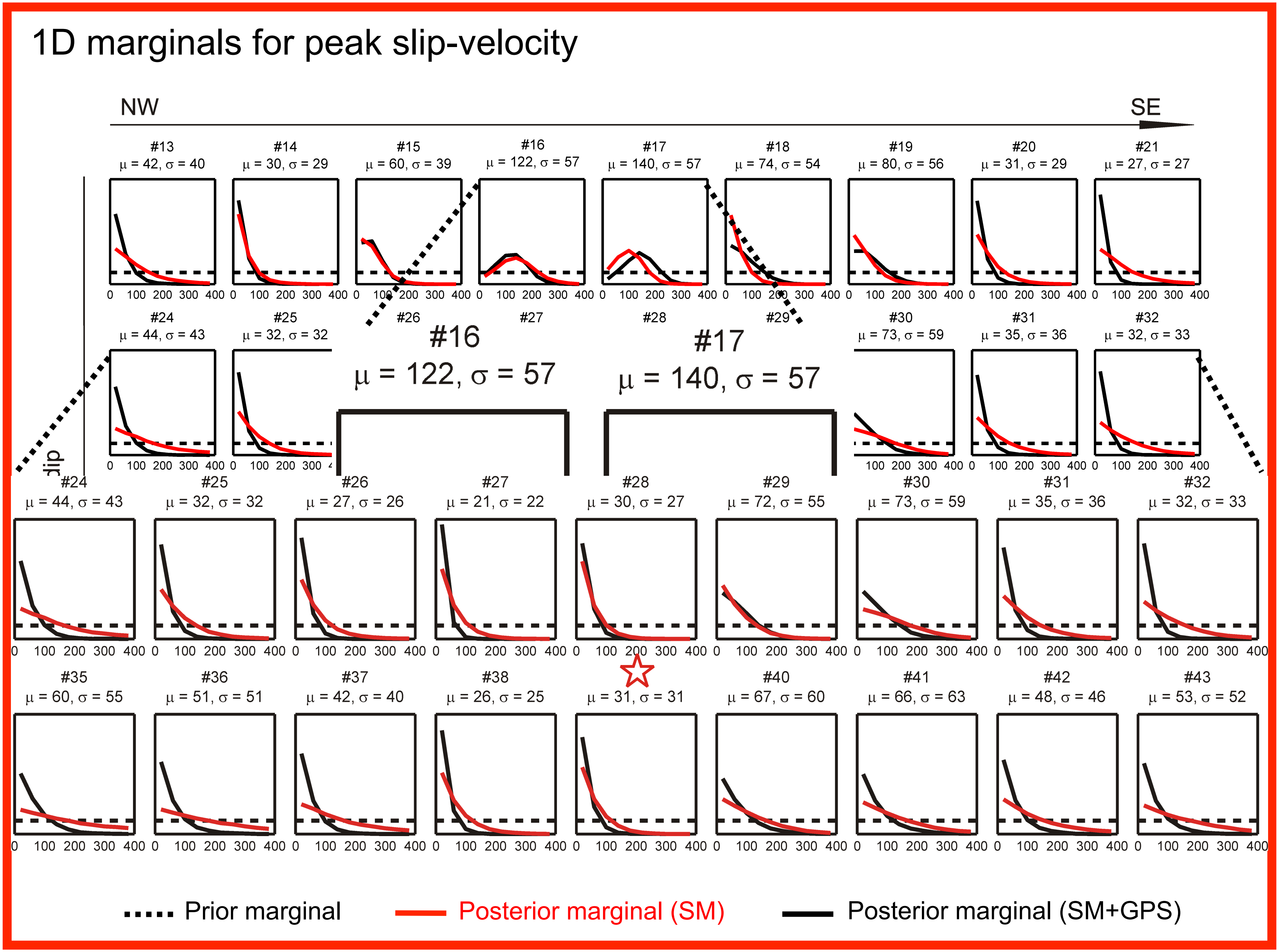
1D marginals for peak slip-velocity
NW
SE
#13 μ = 42, σ = 40
#14 μ = 30, σ = 29
#15 μ = 60, σ = 39
#16 μ = 122, σ = 57
#17 μ = 140, σ = 57
#18 μ = 74, σ = 54
#19 μ = 80, σ = 56
#20 μ = 31, σ = 29
#21 μ = 27, σ = 27
#24 μ = 44, σ = 43
#25 μ = 32, σ = 32
#26
#27
#28
#29
#30 μ = 73, σ = 59
#31 μ = 35, σ = 36
#32 μ = 32, σ = 33
#16 μ = 122, σ = 57
#17 μ = 140, σ = 57
#24 μ = 44, σ = 43
#25 μ = 32, σ = 32
#26 μ = 27, σ = 26
#27 μ = 21, σ = 22
#28 μ = 30, σ = 27
#29 μ = 72, σ = 55
#30 μ = 73, σ = 59
#31 μ = 35, σ = 36
#32 μ = 32, σ = 33
#35 μ = 60, σ = 55
#36 μ = 51, σ = 51
#37 μ = 42, σ = 40
#38 μ = 26, σ = 25
μ = 31, σ = 31
#40 μ = 67, σ = 60
#41 μ = 66, σ = 63
#42 μ = 48, σ = 46
#43 μ = 53, σ = 52
0 100 200 300 400
Prior marginal
Posterior marginal (SM)
Posterior marginal (SM+GPS)

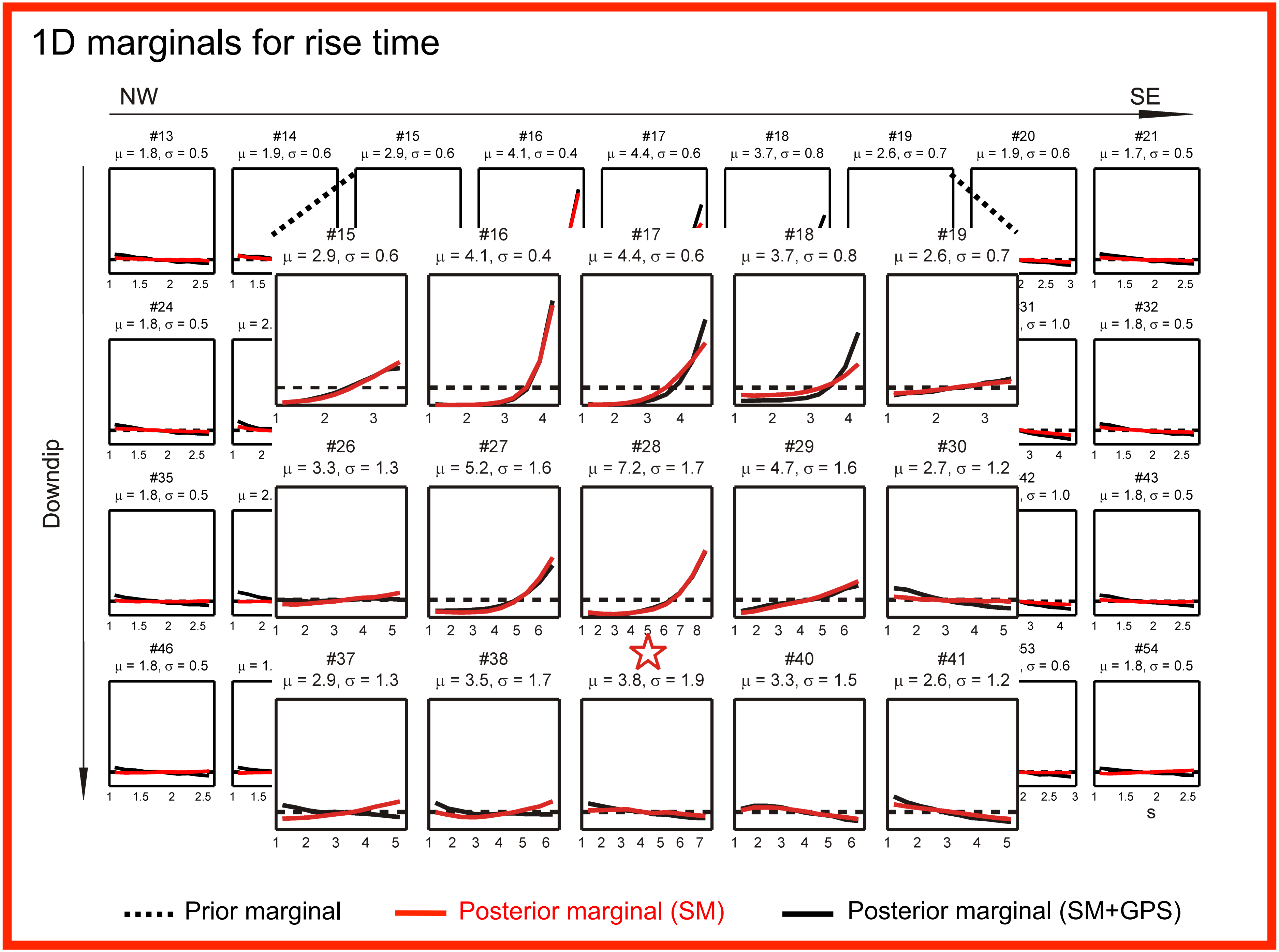
1D marginals for rise time
NW
SE
Downdip
#15
μ = 2.9, σ = 0.6
#16
μ = 4.1, σ = 0.4
#17
μ = 4.4, σ = 0.6
#18
μ = 3.7, σ = 0.8
#19
μ = 2.6, σ = 0.7
#26
μ = 3.3, σ = 1.3
#27
μ = 5.2, σ = 1.6
#28
μ = 7.2, σ = 1.7
#29
μ = 4.7, σ = 1.6
#30
μ = 2.7, σ = 1.2
#37
μ = 2.9, σ = 1.3
#38
μ = 3.5, σ = 1.7
μ = 3.8, σ = 1.9
#40
μ = 3.3, σ = 1.5
#41
μ = 2.6, σ = 1.2
#13
μ = 1.8, σ = 0.5
#14
μ = 1.9, σ = 0.6
#20
μ = 1.9, σ = 0.6
#21
μ = 1.7, σ = 0.5
#24
μ = 1.8, σ = 0.5
#32
μ = 1.8, σ = 0.5
#35
μ = 1.8, σ = 0.5
#43
μ = 1.8, σ = 0.5
#46
μ = 1.8, σ = 0.5
#54
μ = 1.8, σ = 0.5
s
Prior marginal
Posterior marginal (SM)
Posterior marginal (SM+GPS)

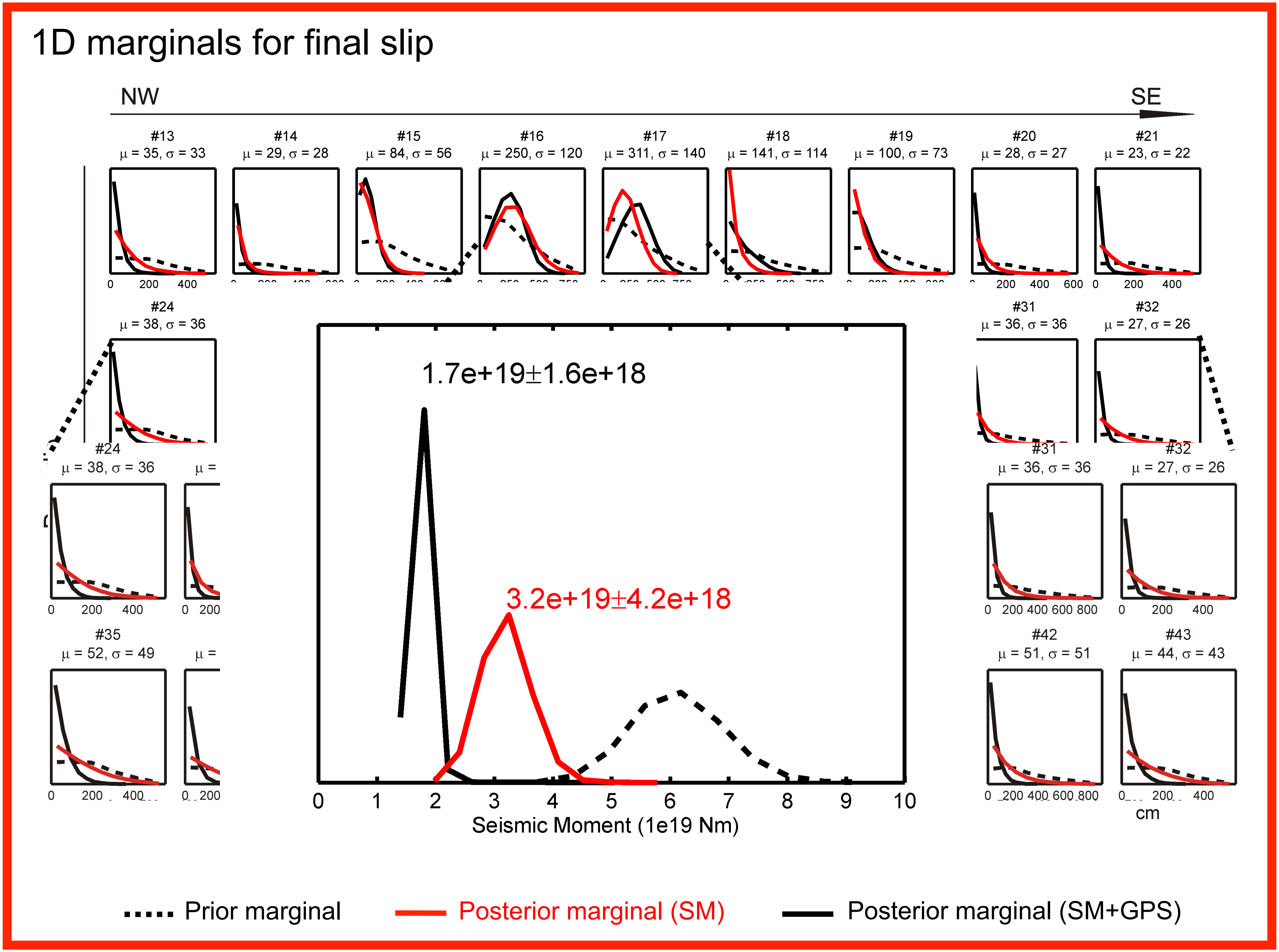
1D marginals for final slip
NW
SE
#13 μ = 35, σ = 33
#14 μ = 29, σ = 28
#15 μ = 84, σ = 56
#16 μ = 250, σ = 120
#17 μ = 311, σ = 140
#18 μ = 141, σ = 114
#19 μ = 100, σ = 73
#20 μ = 28, σ = 27
#21 μ = 23, σ = 22
#24 μ = 38, σ = 36
#31 μ = 36, σ = 36
#32 μ = 27, σ = 26
#35 μ = 52, σ = 49
#42 μ = 51, σ = 51
#43 μ = 44, σ = 43
cm
1.7e+19±1.6e+18
3.2e+19±4.2e+18
Seismic Moment (1e19 Nm)
Prior marginal
Posterior marginal (SM)
Posterior marginal (SM+GPS)

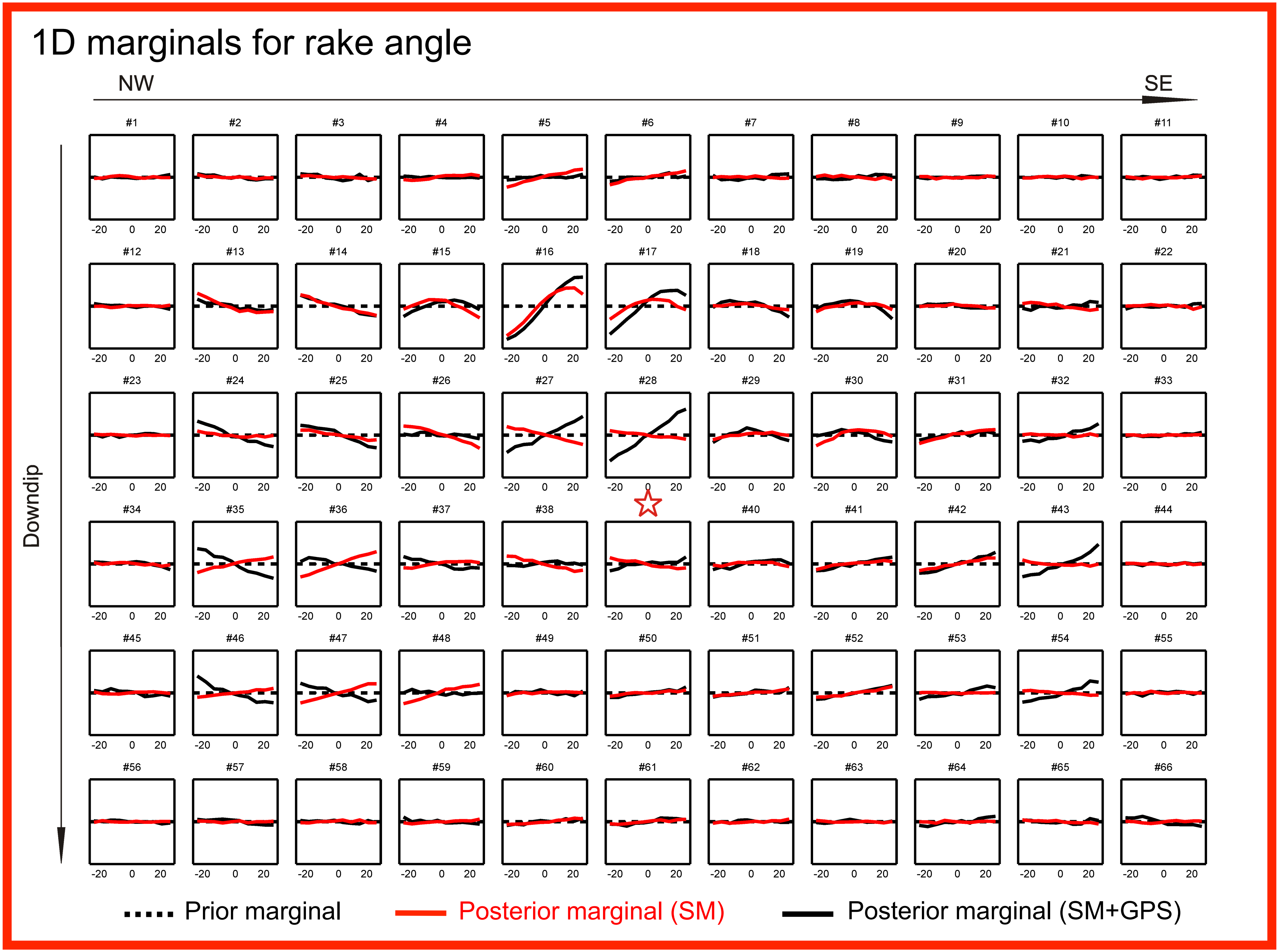
1D marginals for rake angle
NW
SE
Downdip
#1 #2 #3 #4 #5 #6 #7 #8 #9 #10 #11
#12 #13 #14 #15 #16 #17 #18 #19 #20 #21 #22
#23 #24 #25 #26 #27 #28 #29 #30 #31 #32 #33
#34 #35 #36 #37 #38 #40 #41 #42 #43 #44
#45 #46 #47 #48 #49 #50 #51 #52 #53 #54 #55
#56 #57 #58 #59 #60 #61 #62 #63 #64 #65 #66
-20 0 20
Prior marginal
Posterior marginal (SM)
Posterior marginal (SM+GPS)

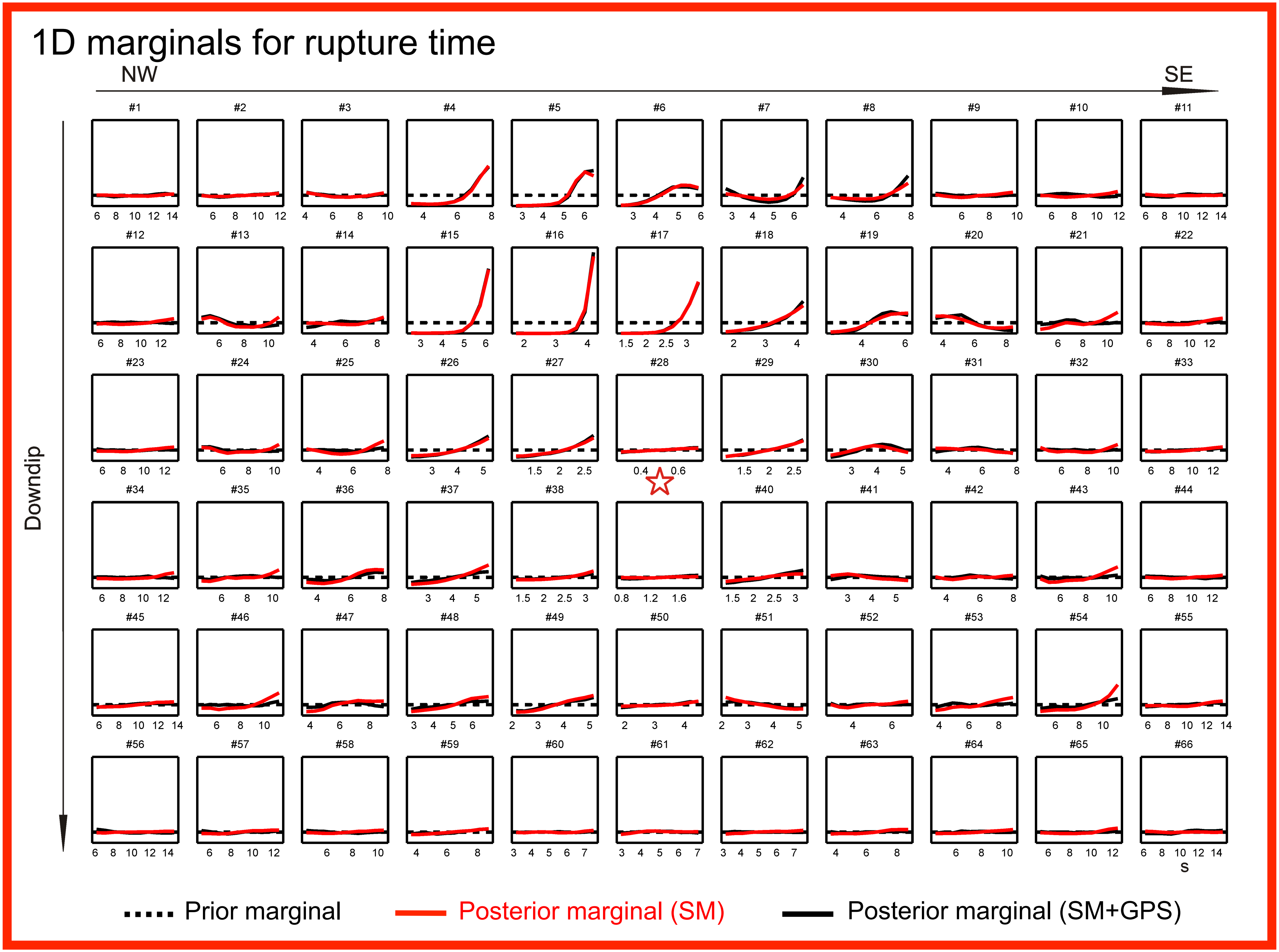
1D marginals for rupture time
NW
SE
Downdip
s
Prior marginal
Posterior marginal (SM)
Posterior marginal (SM+GPS)

Previous studies

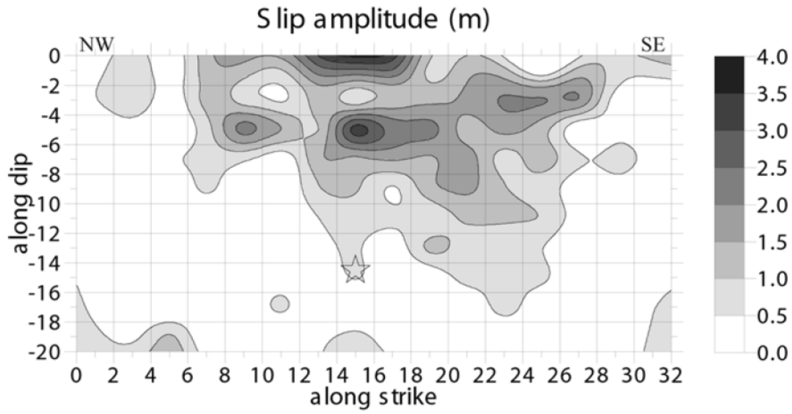

(Semmane et al., 2005)

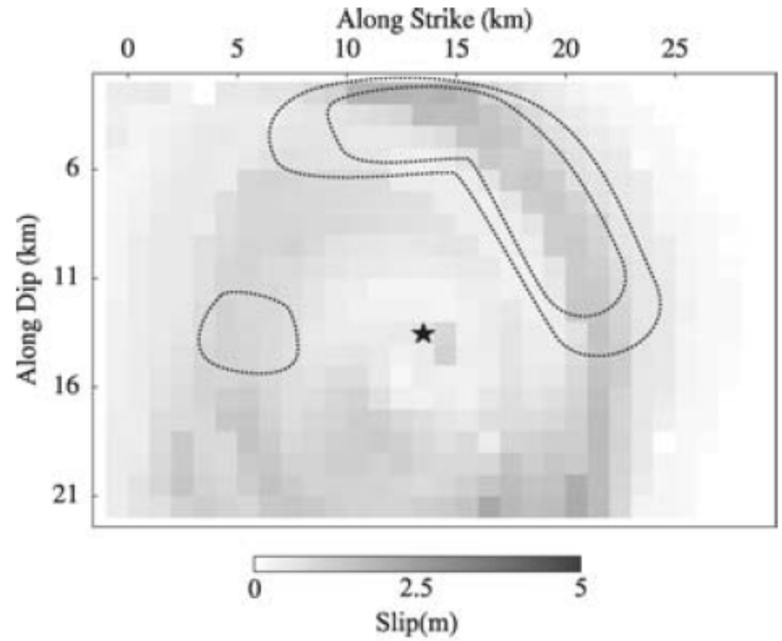

(Festa and Zollo, 2006)

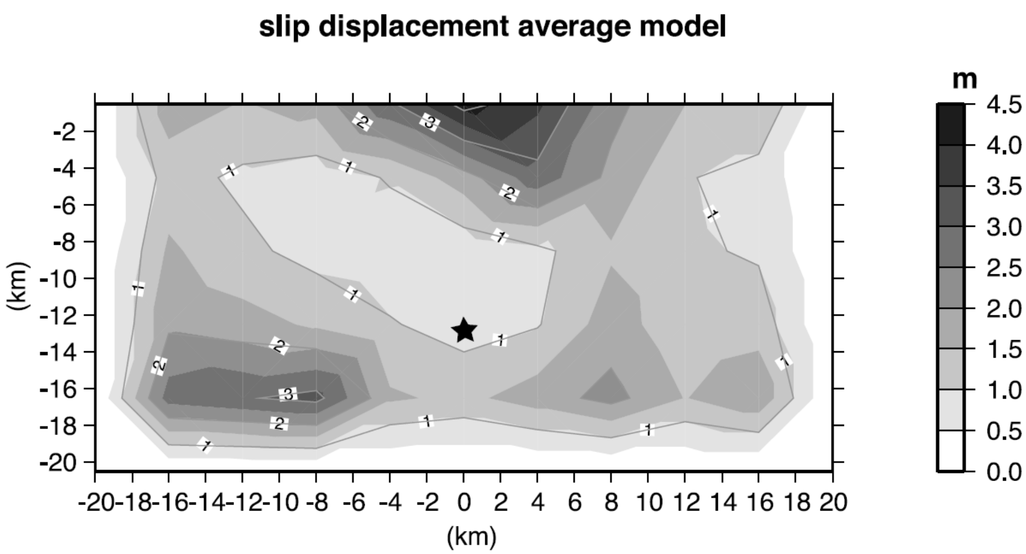

(Piatanesi et al., 2007)

Fit with waveforms

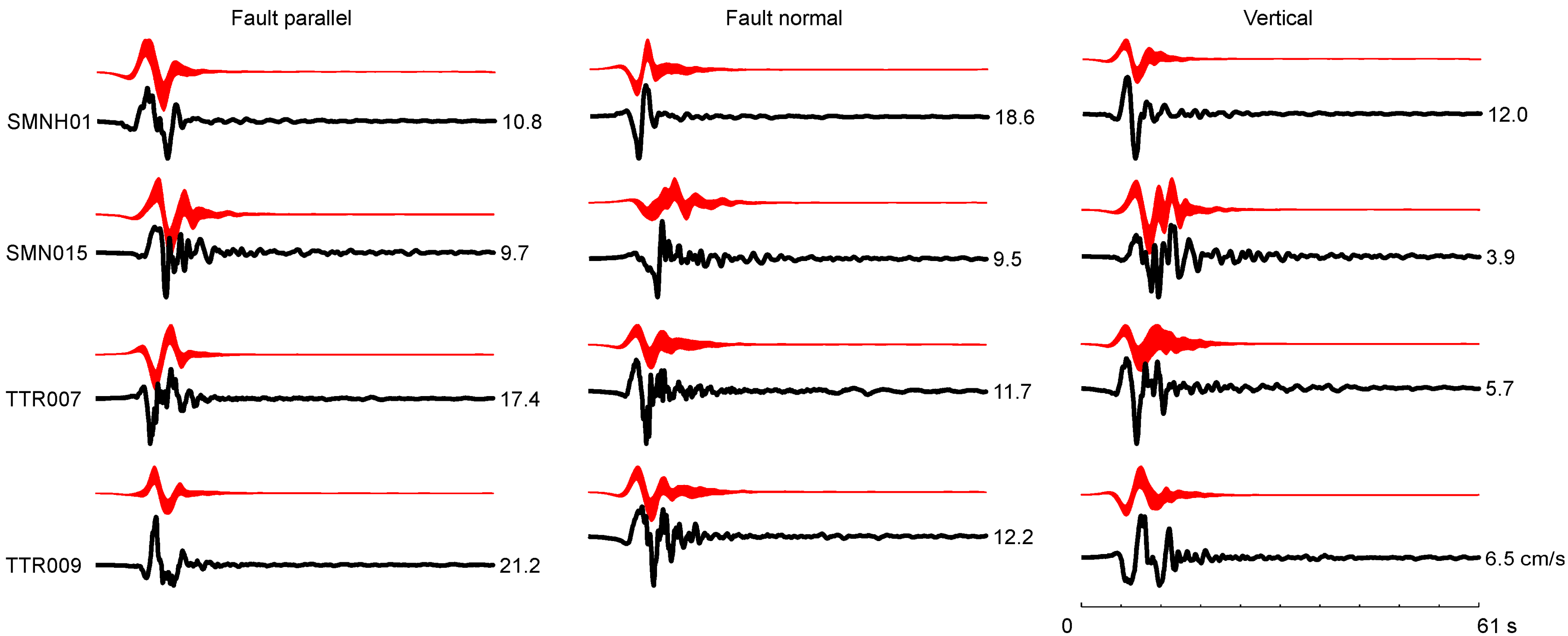

Observations

95% confidence interval of data predictions
(from a set of 3000 kinematic models
fitting both SM and GPS data)

Fit with GPS data

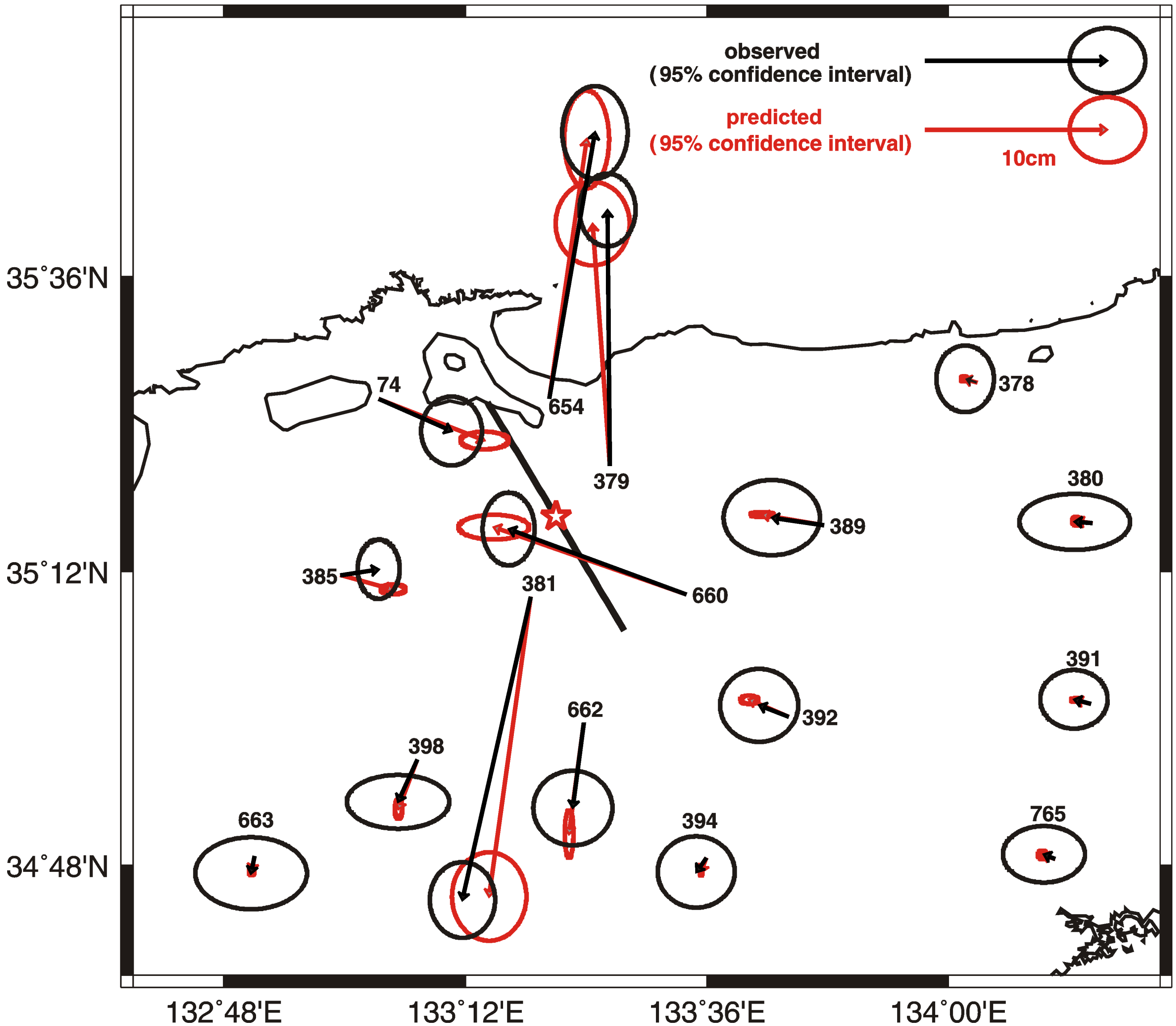

Inversion set-up (2)

Identical to inversion 1 except:

✓Smaller fault plane (length = 24 km, width = 16 km).

✓ Larger model space:

• Range angle can vary between -90 and +90 degrees (previous limits were -30 and +30 degrees)

• Rupture time is determined by two limiting rupture velocities equal to 1 and 4 km/s (previous limits were 1.5 and 4 km/s).

• Rise time can vary between 1 and 10 s. (previous inversion assumed the maximum rise time to decrease approaching the fault edges).

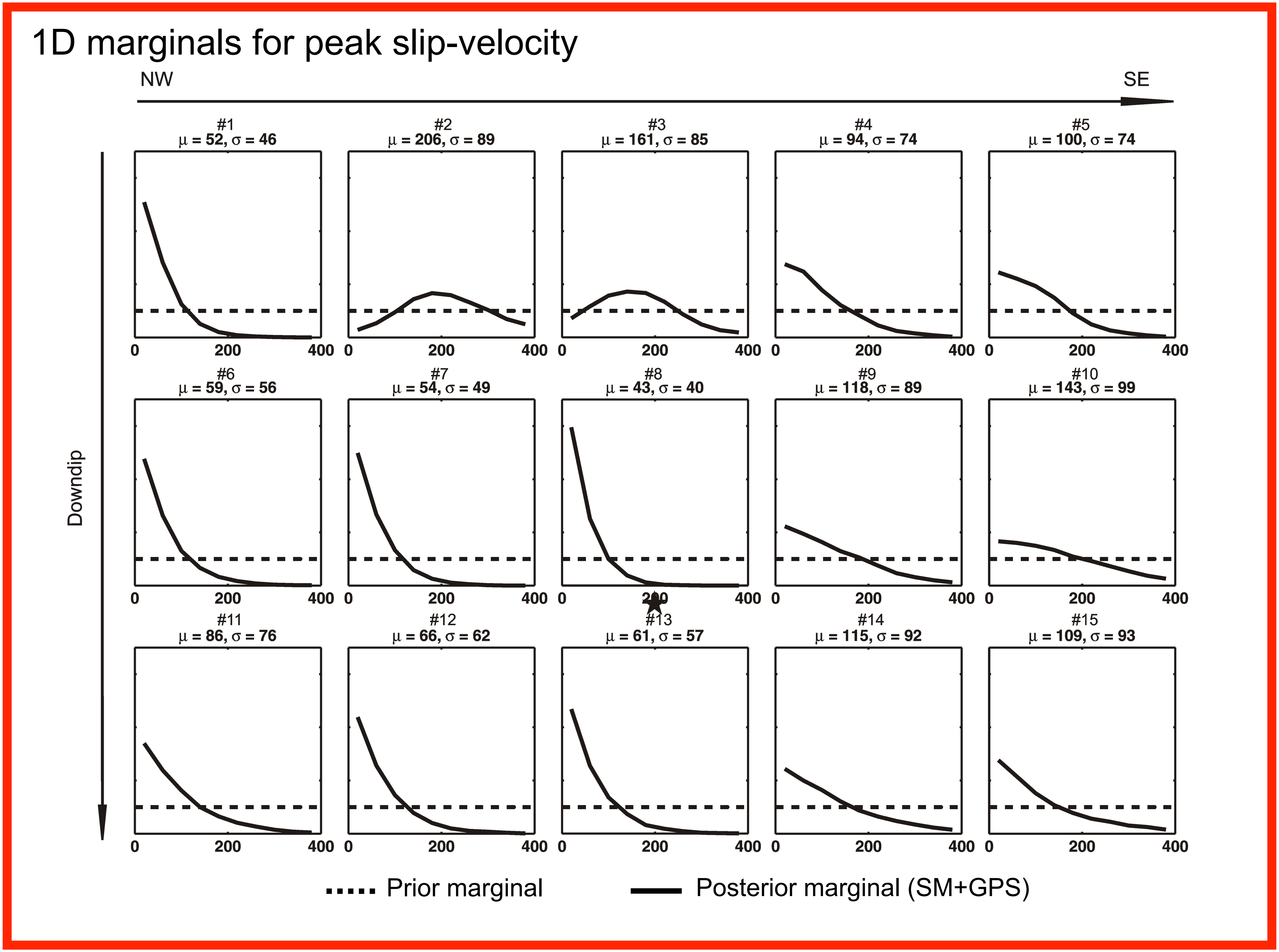

1D marginals for peak slip-velocity
NW
SE
Downdip
#1
μ = 52, σ = 46
#2
μ = 206, σ = 89
#3
μ = 161, σ = 85
#4
μ = 94, σ = 74
#5
μ = 100, σ = 74
#6
μ = 59, σ = 56
#7
μ = 54, σ = 49
#8
μ = 43, σ = 40
#9
μ = 118, σ = 89
#10
μ = 143, σ = 99
#11
μ = 86, σ = 76
#12
μ = 66, σ = 62
#13
μ = 61, σ = 57
#14
μ = 115, σ = 92
#15
μ = 109, σ = 93
0
200
400
Prior marginal
Posterior marginal (SM+GPS)

1D marginals for rake angle

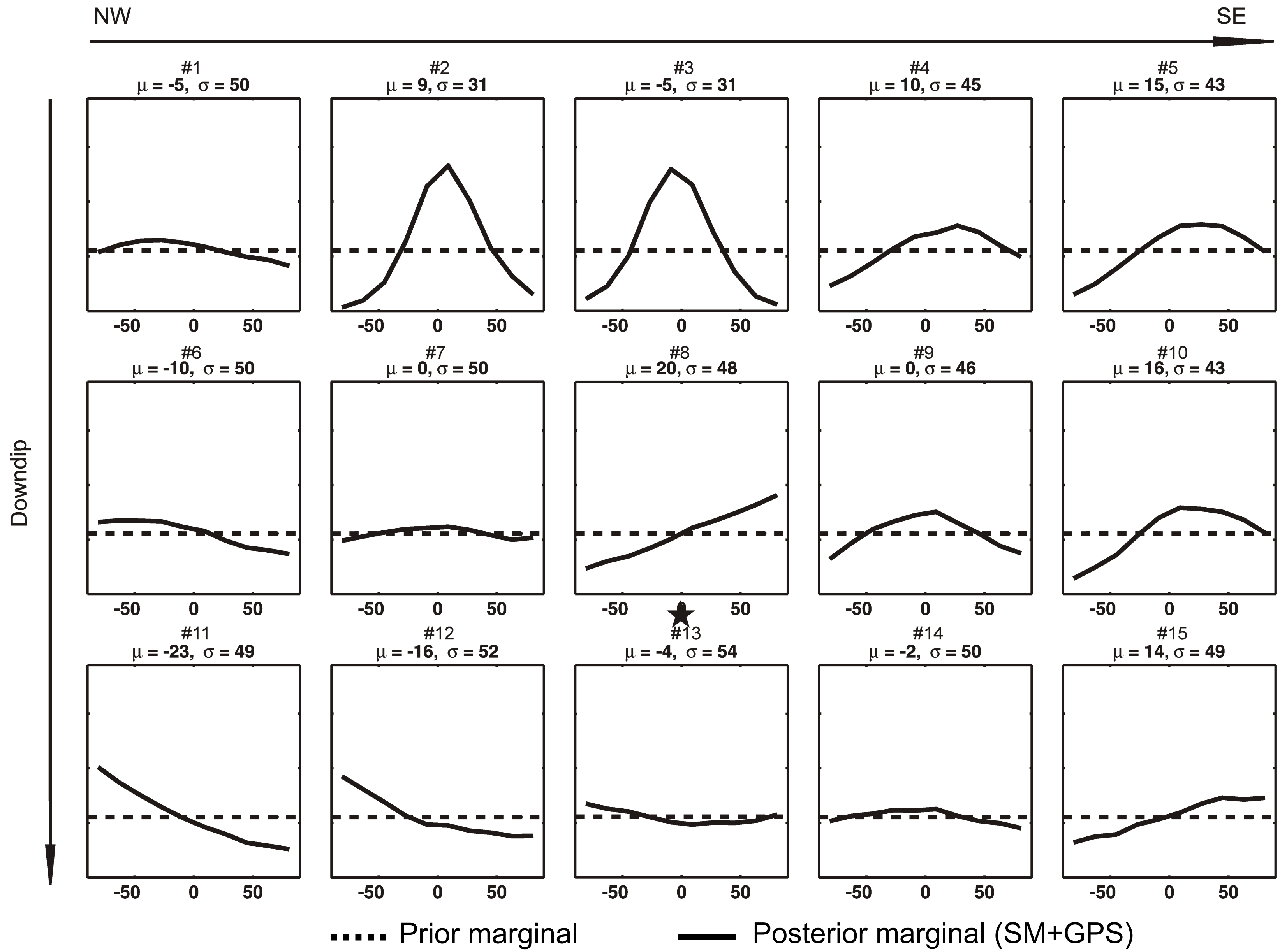

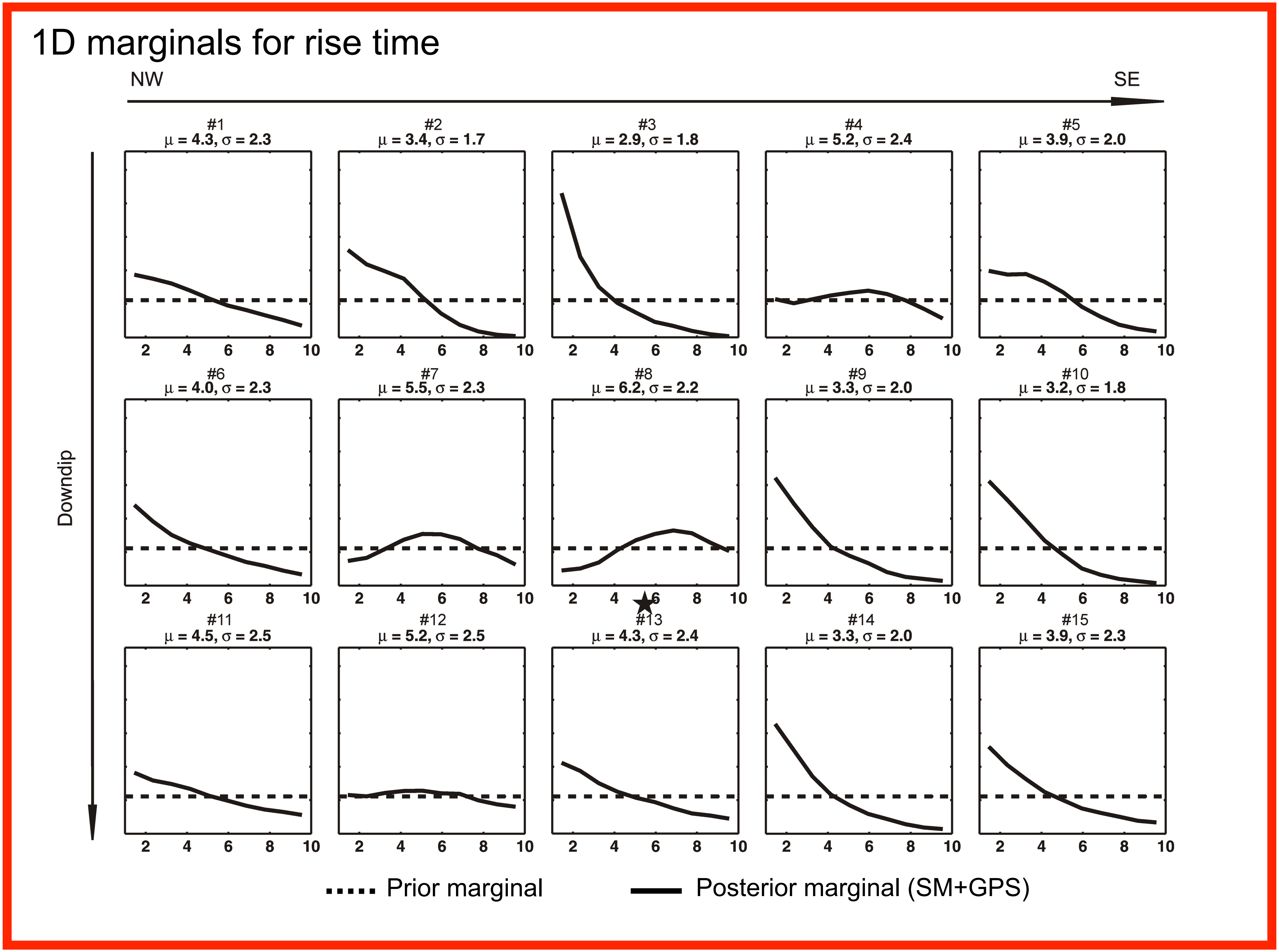
1D marginals for rise time
NW
SE
Downdip
#1
μ = 4.3, σ = 2.3
#2
μ = 3.4, σ = 1.7
#3
μ = 2.9, σ = 1.8
#4
μ = 5.2, σ = 2.4
#5
μ = 3.9, σ = 2.0
#6
μ = 4.0, σ = 2.3
#7
μ = 5.5, σ = 2.3
#8
μ = 6.2, σ = 2.2
#9
μ = 3.3, σ = 2.0
#10
μ = 3.2, σ = 1.8
#11
μ = 4.5, σ = 2.5
#12
μ = 5.2, σ = 2.5
#13
μ = 4.3, σ = 2.4
#14
μ = 3.3, σ = 2.0
#15
μ = 3.9, σ = 2.3
2 4 6 8 10
Prior marginal
Posterior marginal (SM+GPS)

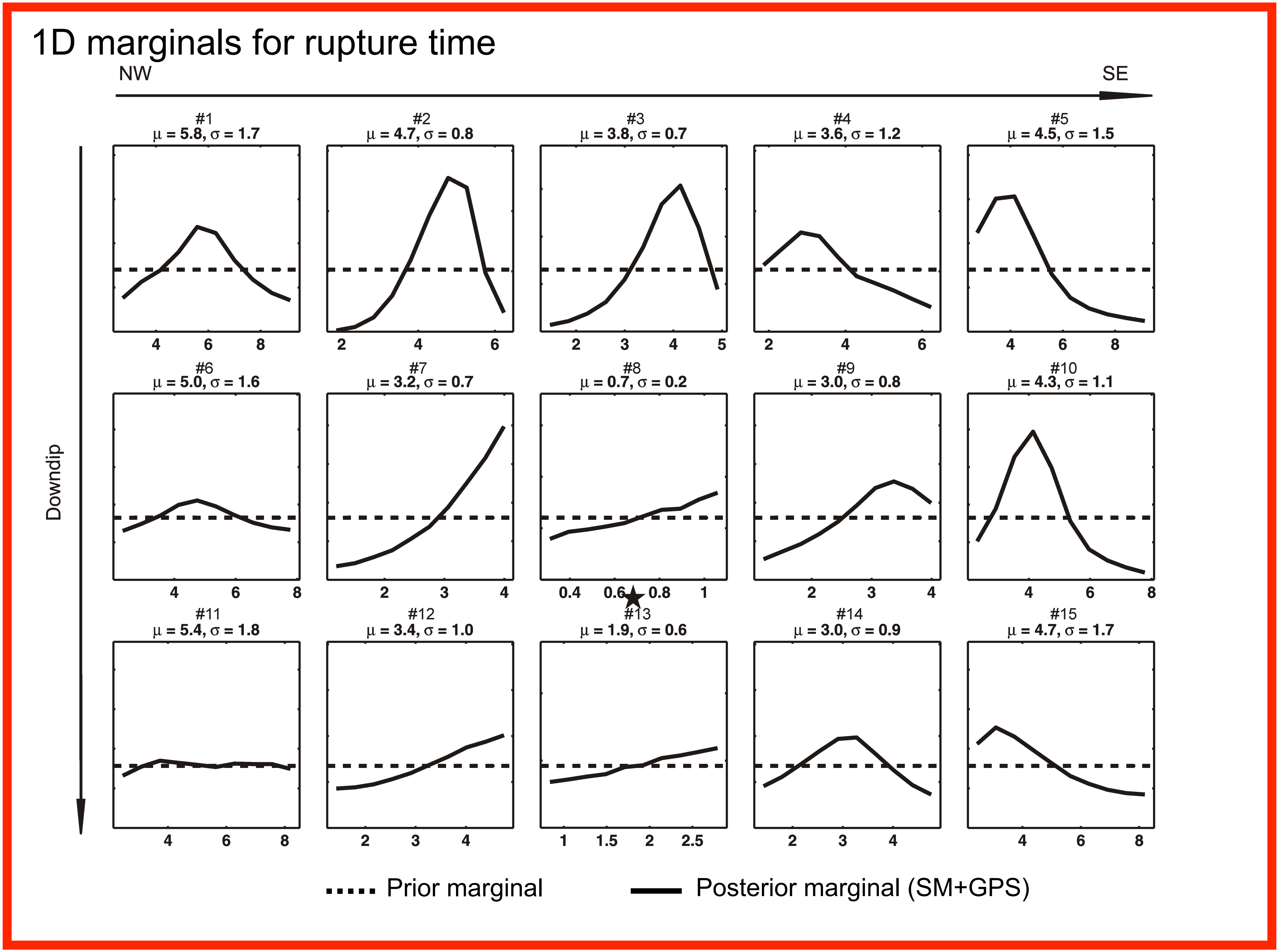
1D marginals for rupture time
NW
SE
Downdip
#1
μ = 5.8, σ = 1.7
#2
μ = 4.7, σ = 0.8
#3
μ = 3.8, σ = 0.7
#4
μ = 3.6, σ = 1.2
#5
μ = 4.5, σ = 1.5
4 6 8
2 4 6
2 3 4 5
2 4 6
4 6 8
#6
μ = 5.0, σ = 1.6
#7
μ = 3.2, σ = 0.7
#8
μ = 0.7, σ = 0.2
#9
μ = 3.0, σ = 0.8
#10
μ = 4.3, σ = 1.1
4 6 8
2 3 4
0.4 0.6 0.8 1
2 3 4
4 6 8
#11
μ = 5.4, σ = 1.8
#12
μ = 3.4, σ = 1.0
#13
μ = 1.9, σ = 0.6
#14
μ = 3.0, σ = 0.9
#15
μ = 4.7, σ = 1.7
4 6 8
2 3 4
1 1.5 2 2.5
2 3 4
4 6 8
Prior marginal
Posterior marginal (SM+GPS)

Conclusions

✓ The Bayesian approach offers a framework for the proper estimation of uncertainties associated with kinematic earthquake rupture parameters, taking into account the full non-linearity of the problem.

✓ The Bayesian approach requires explicit definition of the model space, and helps in understanding if the chosen model space is too limited or not.

✓ In general uncertainties on kinematic rupture parameters are not Gaussian. Actually, Gaussian-like uncertainties identify well resolved features.

General Conclusions

- Multiple kinematic and dynamic earthquake rupture models may provide similar level of fit → robust conclusions should be drawn from ensemble properties

- Bayesian inference is a powerful tool for estimating resolution, which is not possible by using only an optimization algorithm.

- Uncertainties on earthquake rupture parameters are not necessarily Gaussian.

- Uncertainties in kinematic parameters map into dynamic parameters estimates. Correlation between kinematic parameters limits resolution of dynamic parameters.

Conclusions for the Tottori earthquake

- Inferences on final slip for the Tottori earthquake show significant slip between the hypocenter and the top edge of the fault, which is consistent with all previous studies.

- Differently with some previous studies, no significant deep slip is inferred.

- A dynamic model explaining the observed kinematic parameters has been obtained by considering a mean kinematic slip model, and a dynamically consistent source time function (regularized Yoffe function).

- The level of fit provided by the dynamic model is comparable to that of the best-fitting kinematic model obtained through an explicit optimization procedure.

1D marginals for rupture time

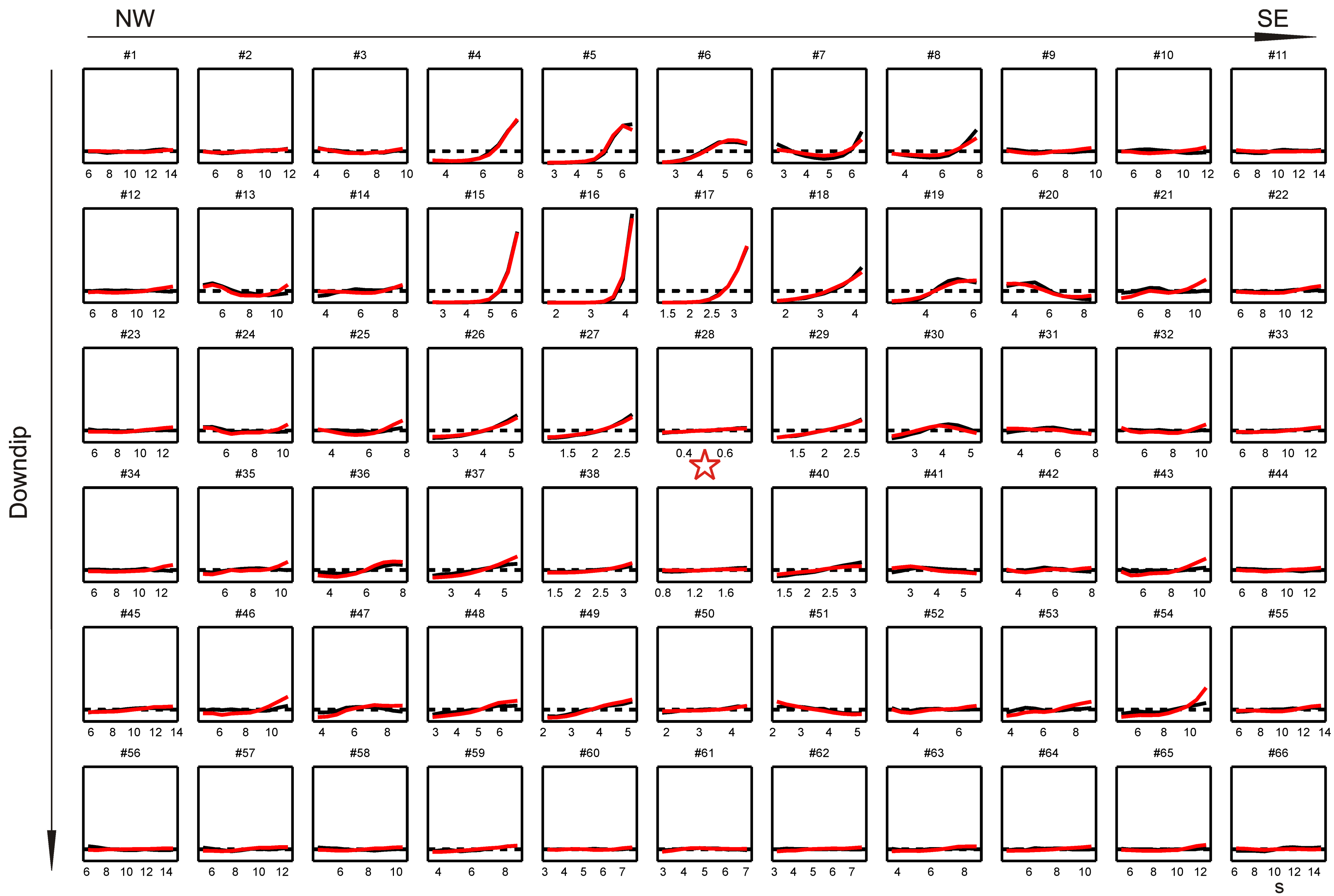

1D marginals for peak slip-velocity

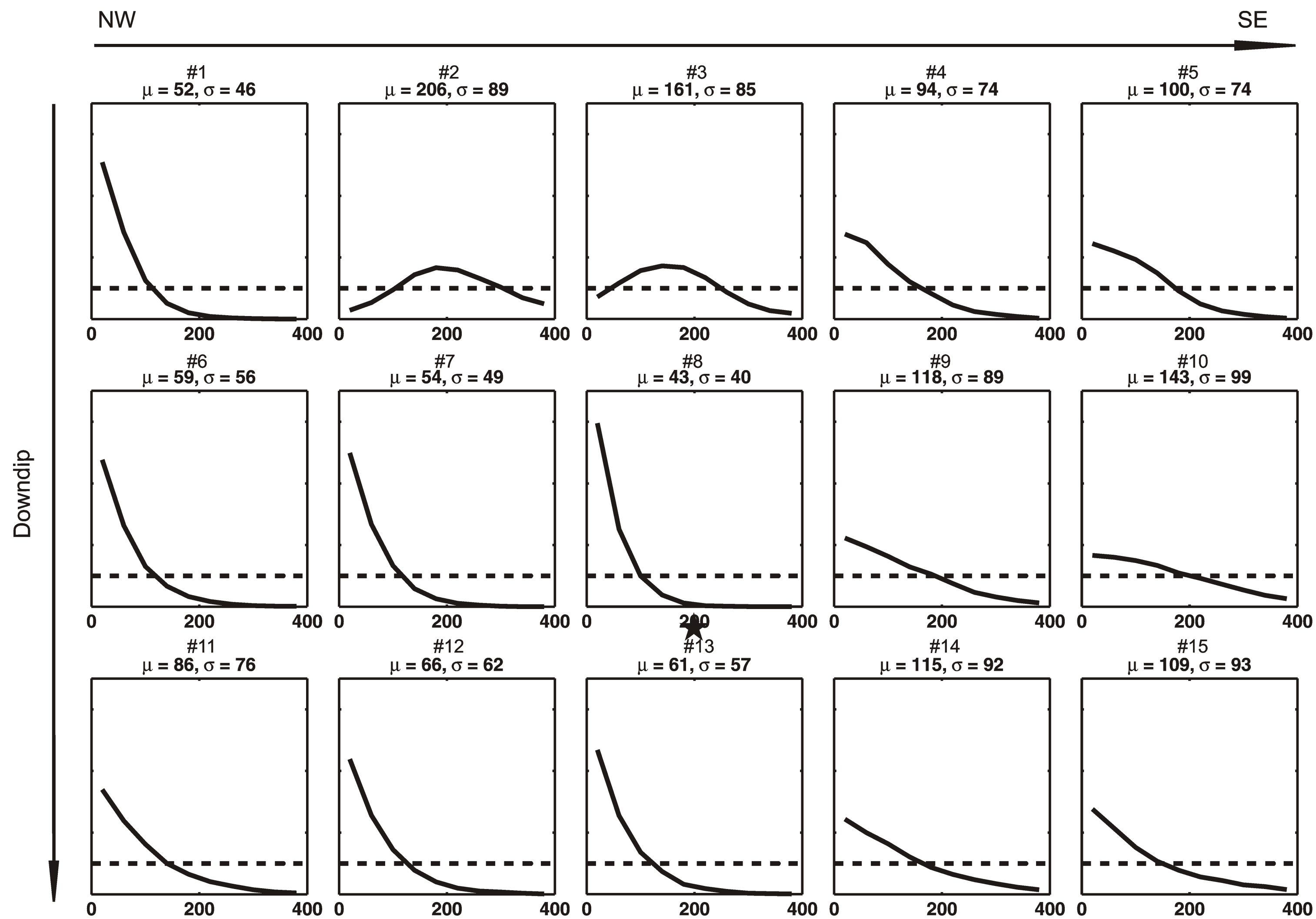

1D marginals for rake angle

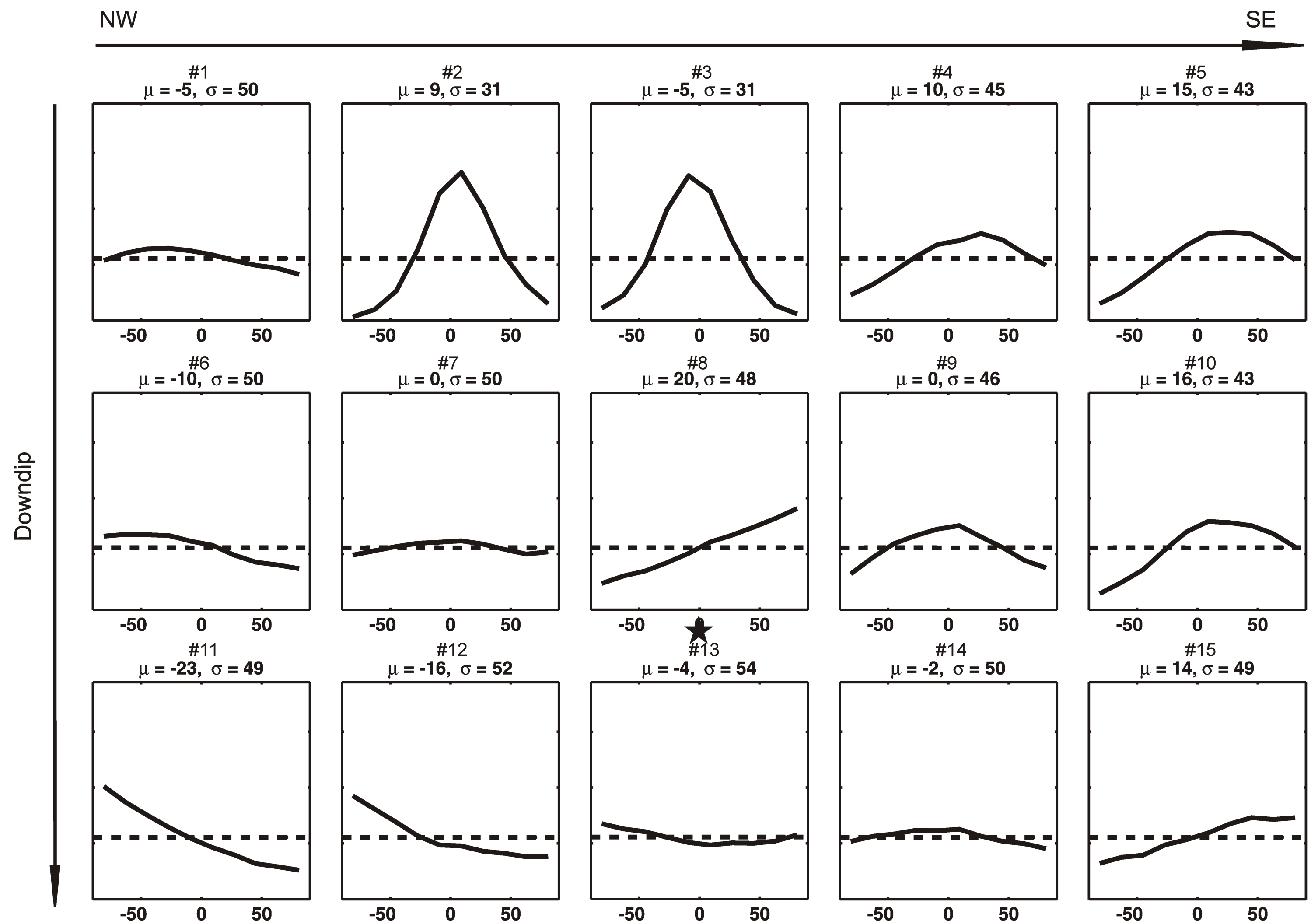

1D marginals for rise time

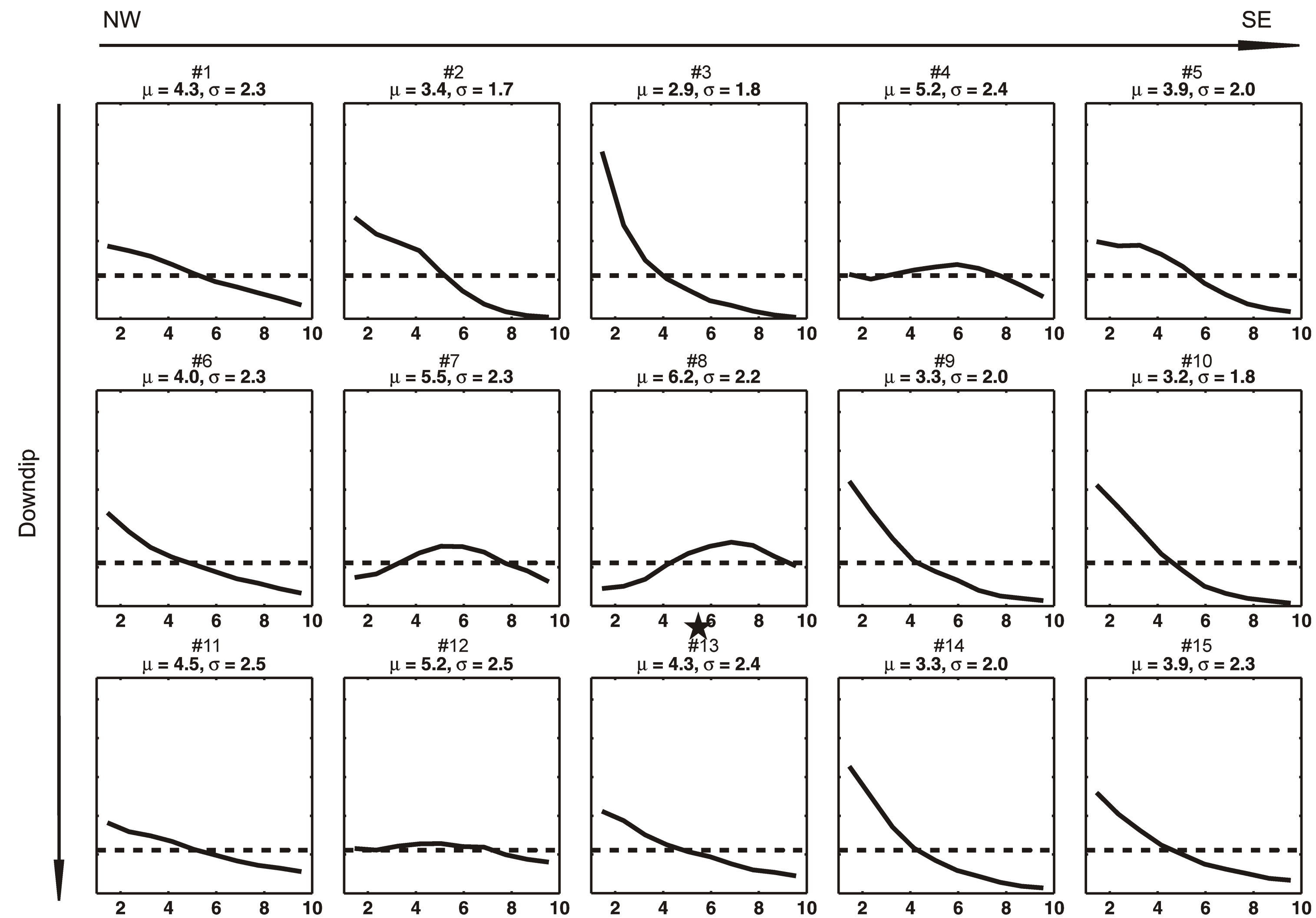

1D marginals for rupture time

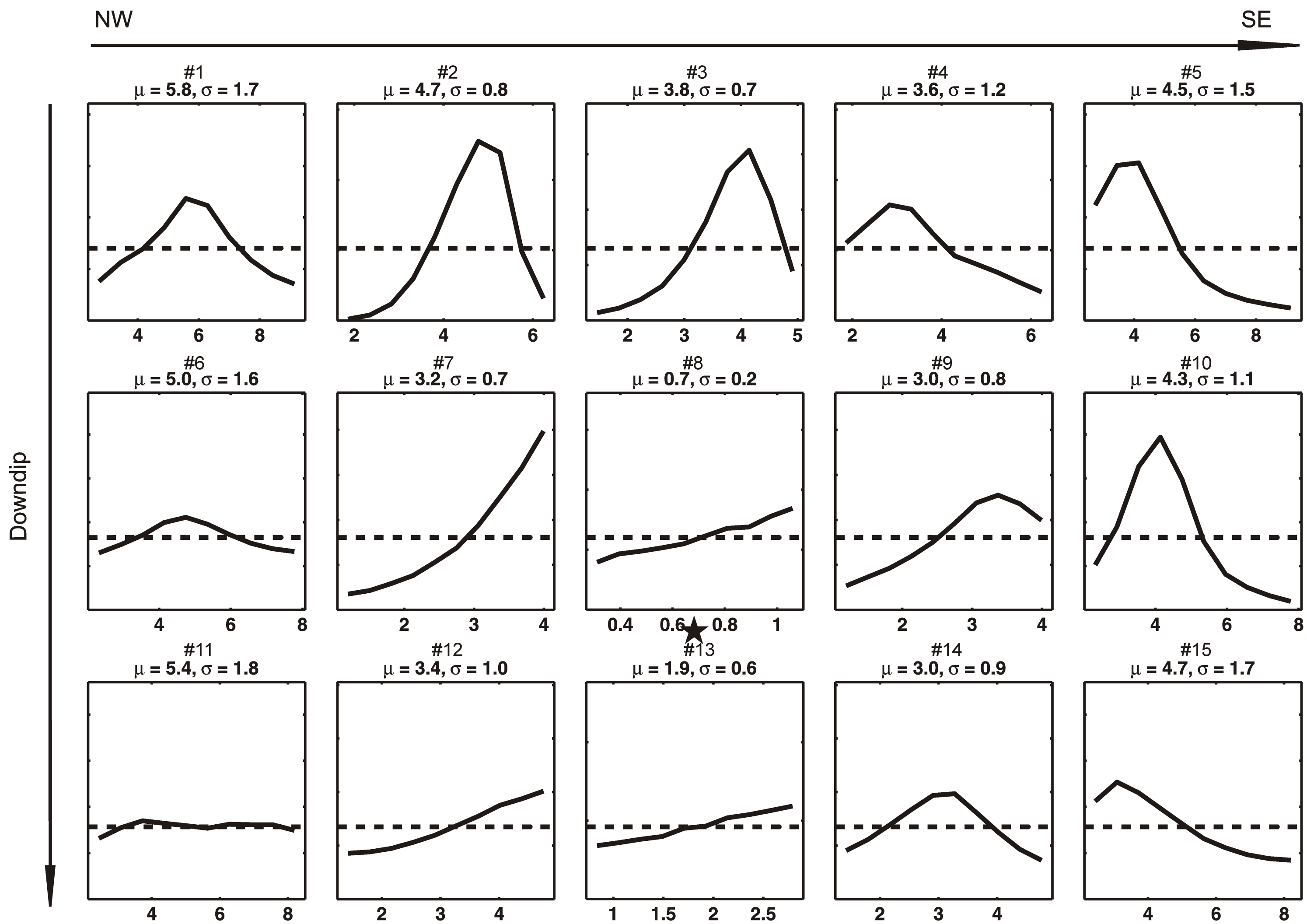

1D marginals for final slip

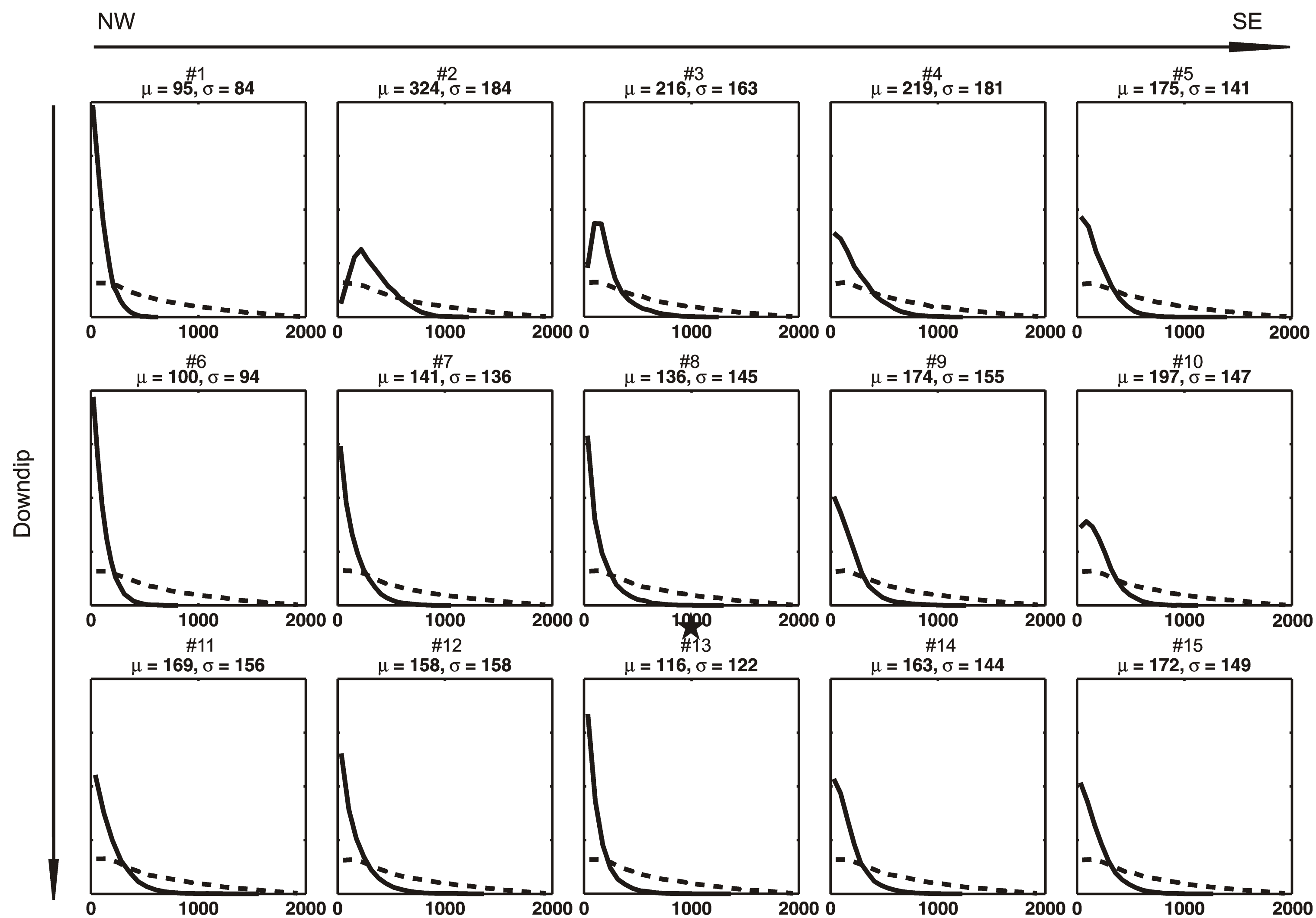

The mean kinematic slip model

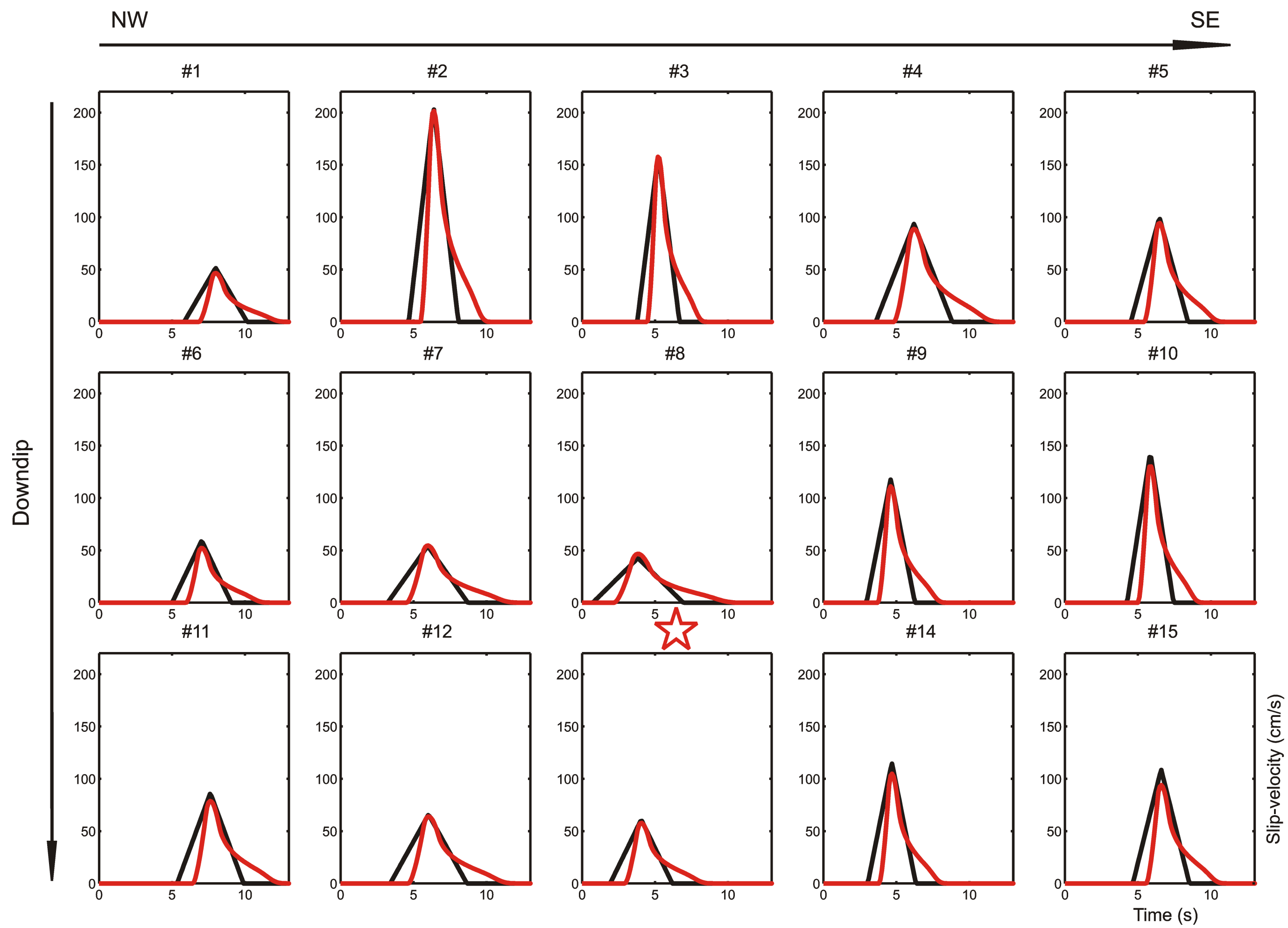

Mean kinematic source time function (isosceles triangle)

Regularized Yoffe function

A LINEAR SLIP-WEAKENING MODEL

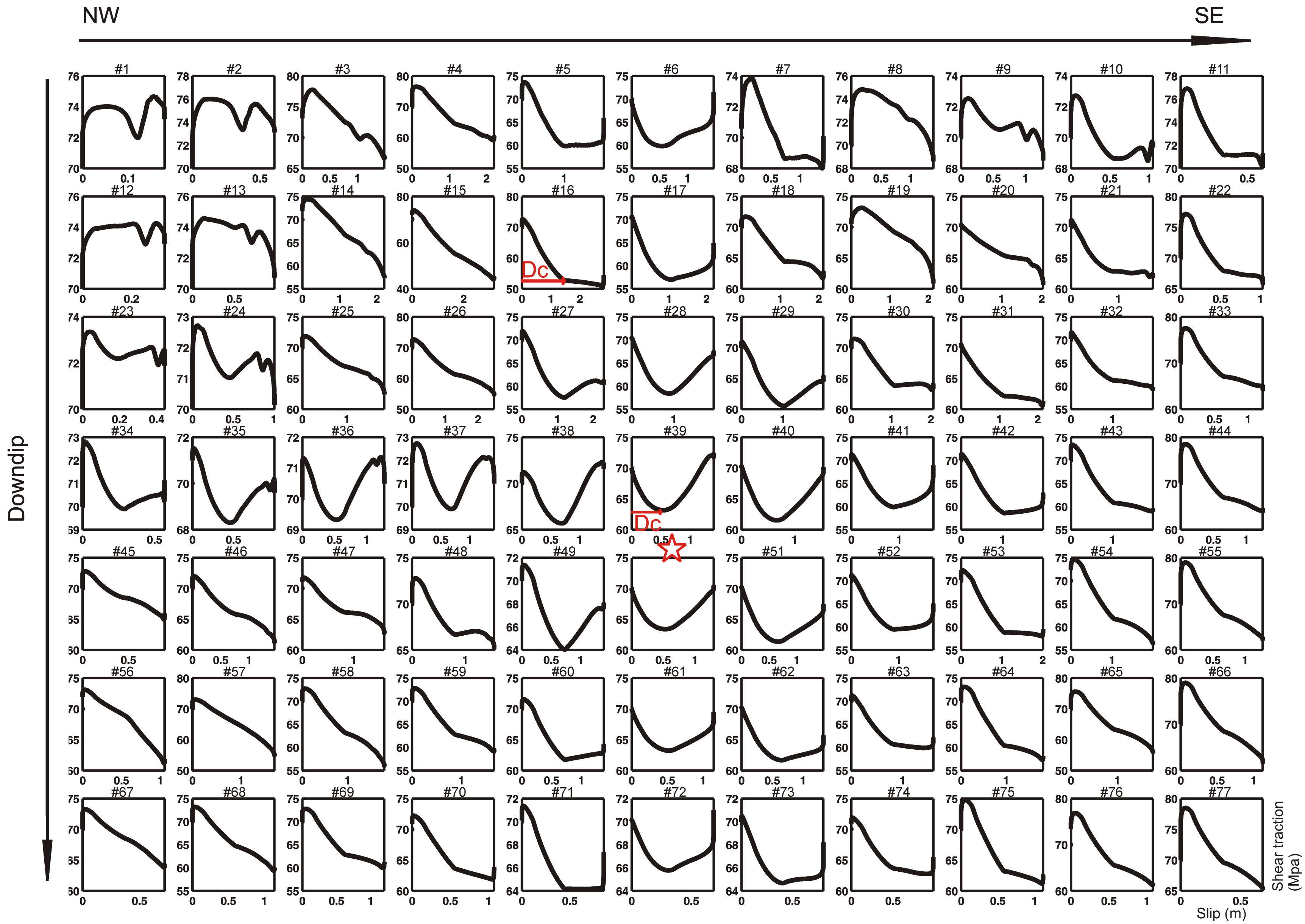

The (geological) earthquake source

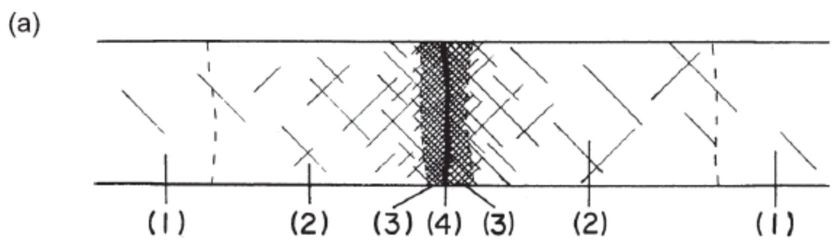

(1) Undamaged host rock
(2) Damage zone, highly cracked; 10s m to 100 m wide, minor faults may reach 1 km
(3) Gouge or foliated gouge; 1 m to 10s m wide
(4) Central ultracataclasite shear zone, may be clay rich; 10s mm to 100s mm wide
(5) [within (4), not marked above] Prominent slip surface; may be < 1 to 5 mm wide

The "fault zone" (Rice and Cocco, 2005)

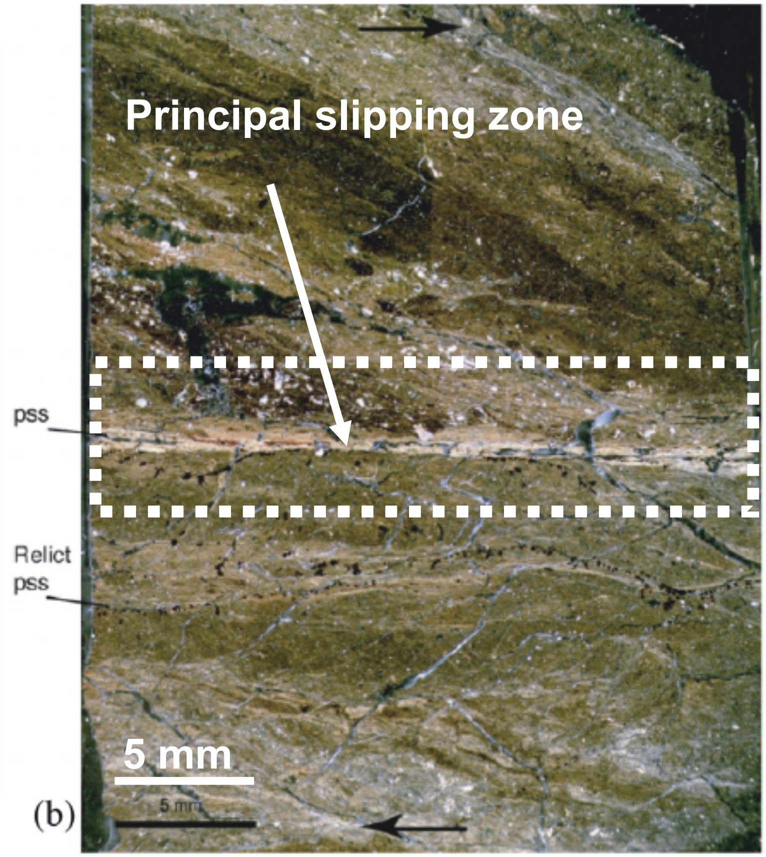

Punchbowl fault (San Andreas fault system), (Rice, 2006)

Static stress drop

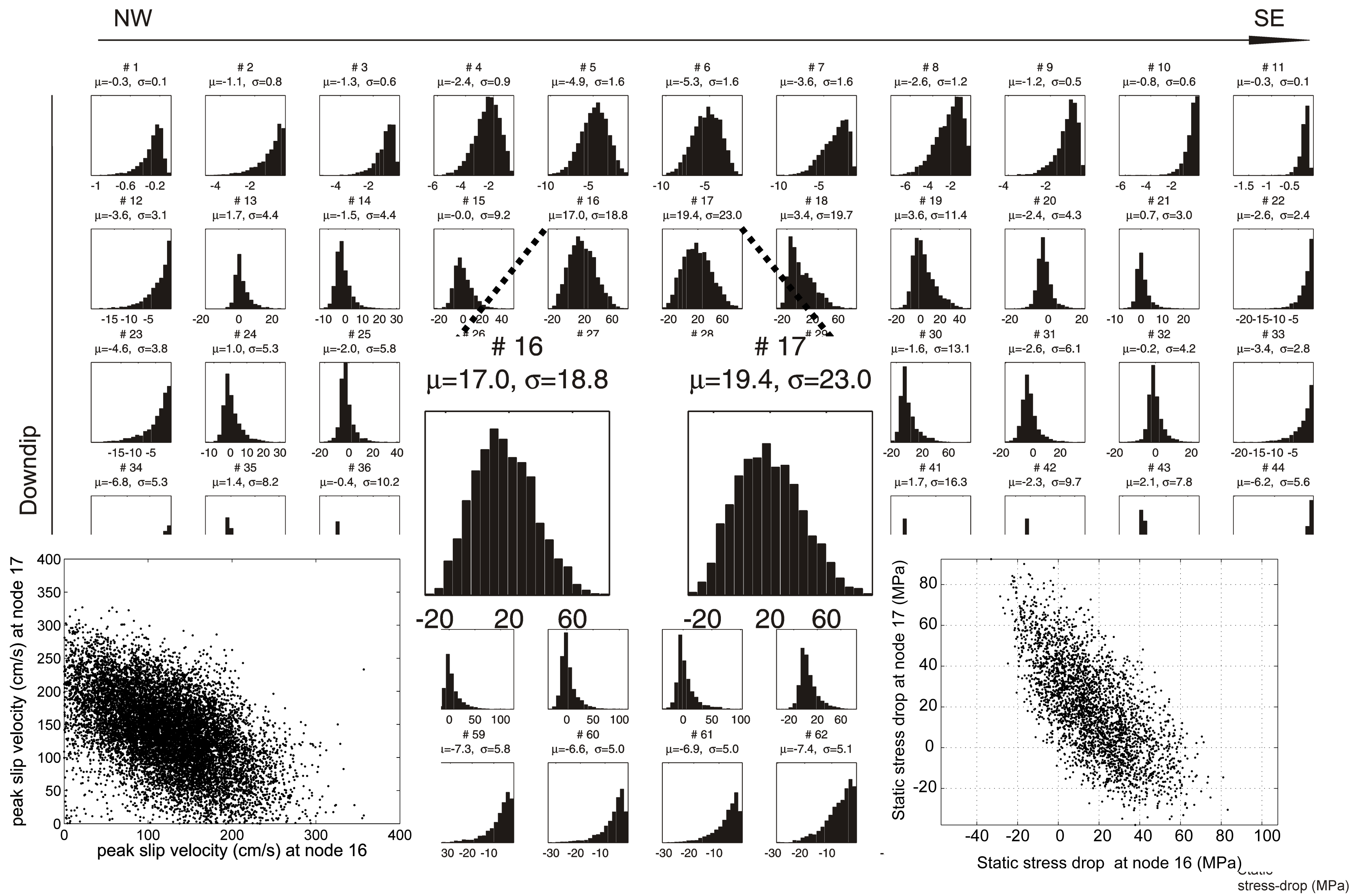

Uncertainties for the Tottori earthquake

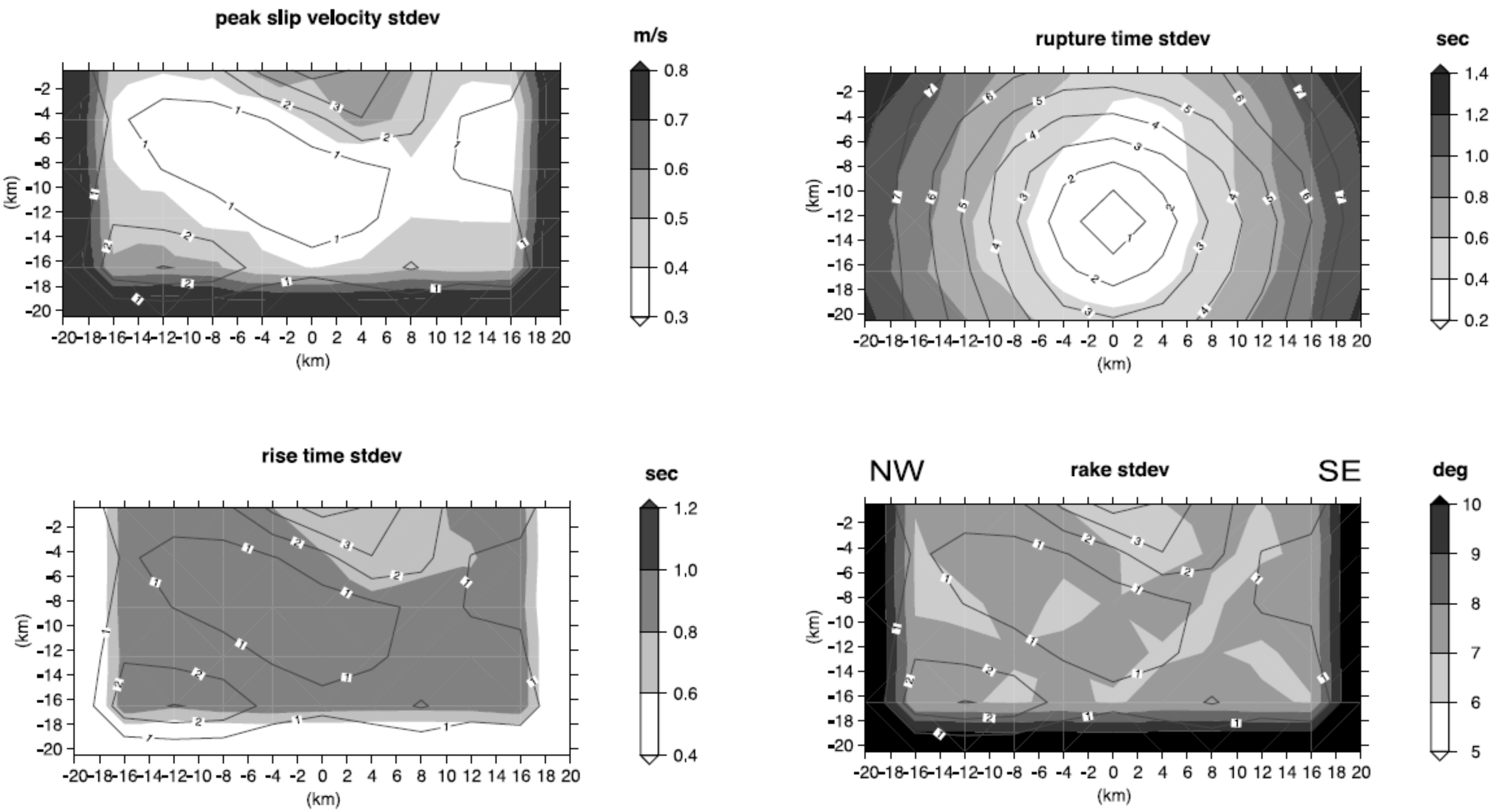

(Piatanesi et al, 2007)

Uncertainties in earthquake images

1989, Loma Prieta earthquake

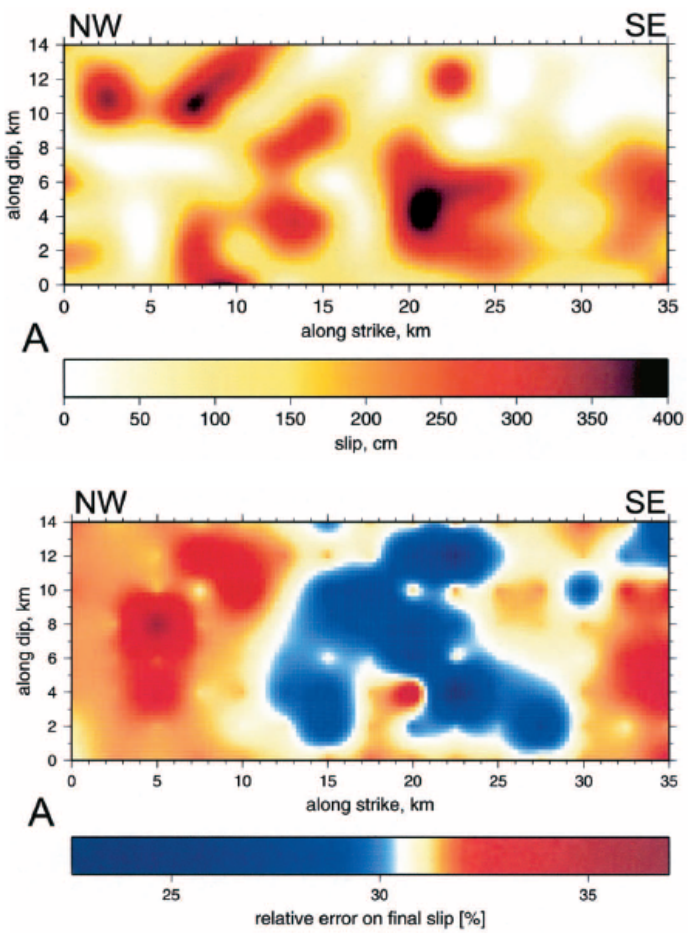

(Emolo and Zollo, 2005)

2000, Western Tottori earthquake

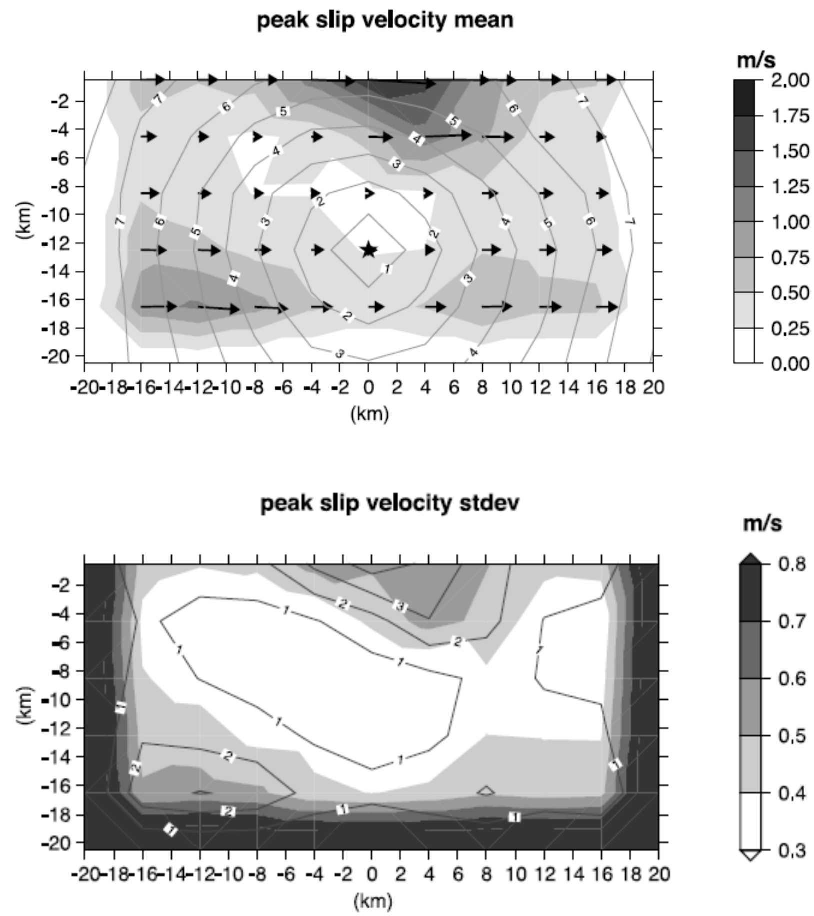

(Piatanesi et al, 2007)